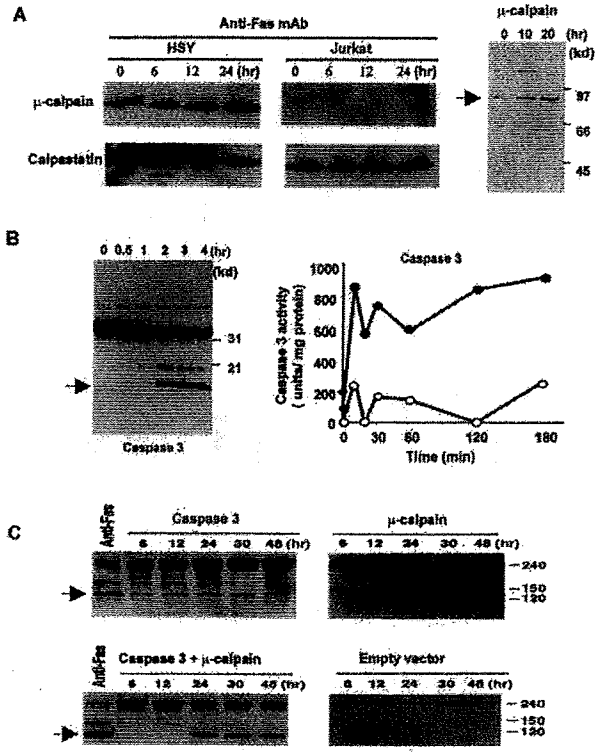

Figure 3. Detection of cysteine proteases in anti-Fas-induced apoptotic HSY cells. Western blot analysis of μ-calpain, and calpastatin in apoptotic HSY and Jurkat cells stimulated with anti-Fas Ab (CH-11). A constitutive expression of μ-calpain, and its time-dependent increase were observed in anti-Fas-stimulated HSY cells. Calpastatin activity is shown to be constitutively expressed.more than calpain expression and a time-dependent decrease of calpastatin expression was observed in apoptotic HSY cells, not in Jurkat cells. **A:** Western blot analysis of the active form of μ-calpain in apoptotic HSY cells stimulated with anti-Fas mAb (CH-11). **B:** Western blot analysis showing a time-dependent increase in caspase 3 and sequential activation of caspase 3-like protease in anti-Fas-induced apoptotic HSY cells. The caspase 3-like activity in the lysates (100 mg protein) (**filled circle**) or in the presence of 50 mmol/L MOCAc-DEVD-NH2 (**open circle**) was determined using fluorescent substrates in apoptotic HSY cells. One unit corresponds to the activity that cleaves 1 pmol of the respective fluorescent substrate at 30°C in 30 minutes. **C:** Detection of cleavage product of 120-kd α-fodrin in co-transfected HSY cells overexpressed with full-length caspase 3 and μ-calpain cDNAs. Analysis of lysates from caspase 3 and μ-calpain cDNA co-transfected cells revealed a fivefold to sevenfold increase of 120-kd α-fodrin in the level of expression of caspase 3 or μ-calpain in cells transfected with each construct.

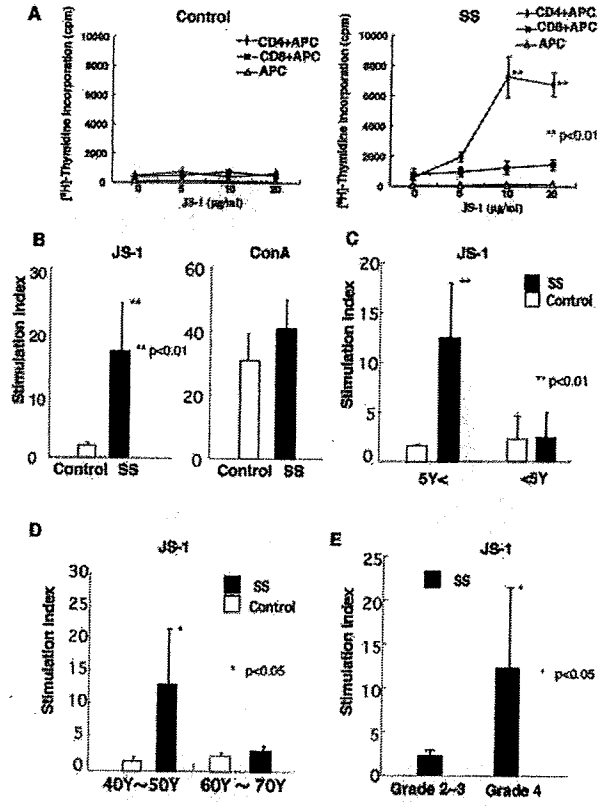

Figure 4. A: Significant proliferative $CD4^+$ T-cell responses, not $CD8^+$ T cells, to the AFN protein (JS-1) in the patients with primary SS ($n = 3$), not in age-matched control ($n = 2$) (**$P < 0.01$, Student's *t*-test). **B:** Significant proliferative responses (stimulation indices > 3) of PBMCs to the AFN protein (JS-1) in patients with primary SS ($n = 14$), not in age-matched control ($n = 11$) (**$P < 0.01$, Student's *t*-test). **C:** Proliferative responses to JS-1 of PBMCs from SS patients with short duration (within 5 years) from the onset of the disease ($n = 8$) were significantly higher than those with long duration (more than 5 years) ($n = 6$) (**$P < 0.01$, Student's *t*-test). **D:** Proliferative responses to JS-1 of PBMCs from younger SS patients (40 to 50 years of age) ($n = 8$) were significantly higher than those with older SS patients (60 to 70 years of age) ($n = 6$) (*$P < 0.05$, Student's *t*-test). **E:** Significant proliferative responses to JS-1 protein were observed in PBMCs from SS patients with higher pathological score ($n = 9$, grade 4) than those with lower score ($n = 5$, grade 2 or grade 3) (*$P < 0.05$, Student's *t*-test). All data are expressed as stimulation indices ± SEM.

PBMCs as antigen-presenting cells. Significant proliferative responses were observed in $CD4^+$ T cells from SS patients, not in $CD8^+$ T cells (Figure 4A). Moreover, it has been determined by flow cytometric analysis that the accumulated population in response to both AFN protein (JS-1) and AFN peptide among PBMCs of SS patients is $CD4^+$ T cell (data not shown). Then, we used PBMCs for the proliferation assay. We found proliferative T-cell responses (stimulation indices > 3) to the AFN protein (JS-1) using PBMCs from 14 of 18 patients with SS, not from age-matched healthy patients ($n = 11$) (Figure 4B). Proliferative responses to JS-1 of SS patients with short duration (within 5 years) from the onset of disease ($n = 8$) were significantly higher than those with long duration (longer than 5 years) ($n = 6$) (Figure 4C). Proliferative responses to JS-1 autoantigen with younger SS patients (40 to 50 years of age) ($n = 8$) were significantly higher than those with older SS patients (60 to 70 years of age) ($n = 6$) (Figure 4D). Significant proliferative responses to JS-1 protein were observed in PBMCs from SS patients with higher pathological score ($n = 9$, grade 4) than those with lower score ($n = 5$, grade 2 or grade 3) (Figure 4E). Synthetic peptides of AFN were generated, and immunoregulatory roles were investigated using PBMCs from patients with SS, compared with SLE and RA. Significant proliferative T-cell responses to AFN peptide were detected in PBMCs from 9 of 18 patients with SS, but not with SLE, RA, and healthy controls (Figure 5). We next analyzed intracellular cytokines using isolated PBMCs (10^6/ml). $CD4^+$ T cells from PBMCs with SS patients induce Th1 cytokine (IL-2, IFN-γ) when pulsed with AFN peptide (10 μg/ml) (Figure 6A), not with control laminin fragment peptide (10 μg/ml). We observed a significant decrease in both $CD4^+$ Fas^+ T and $CD4^+$ $FasL^+$ T cells in SS patients,

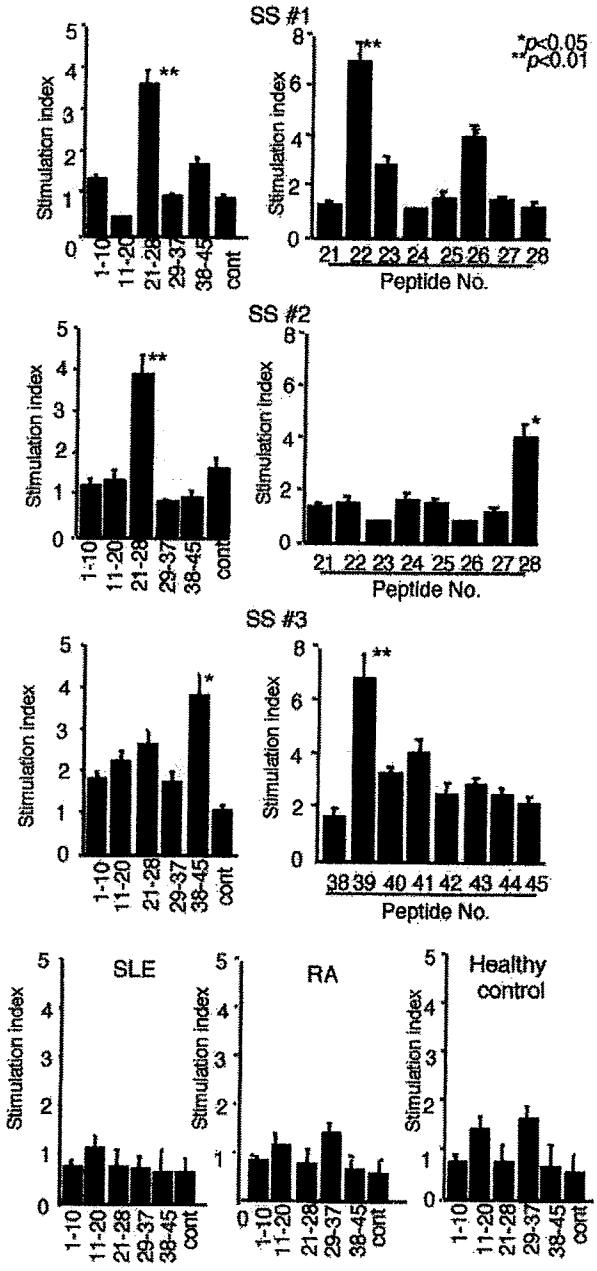

Figure 5. Significant proliferative responses of PBMCs were seen with AFN peptide in the patients with primary SS. Nine of eighteen SS patients examined reacted significantly with single AFN peptide, but not in SLE ($n = 6$), RA ($n = 5$), and age-matched healthy controls ($n = 6$). Representative profiles in three different patients with SS (SS 1, SS 2, SS 3) indicate significant proliferative responses with peptide mixture and individual peptide of p22, p26, p28, and p39 ($^*P < 0.05$, $^{**}P < 0.01$; Student's *t*-test), but not with laminin fragment peptide 929-933 as control antigen. The results are expressed as stimulation indices ± SEM.

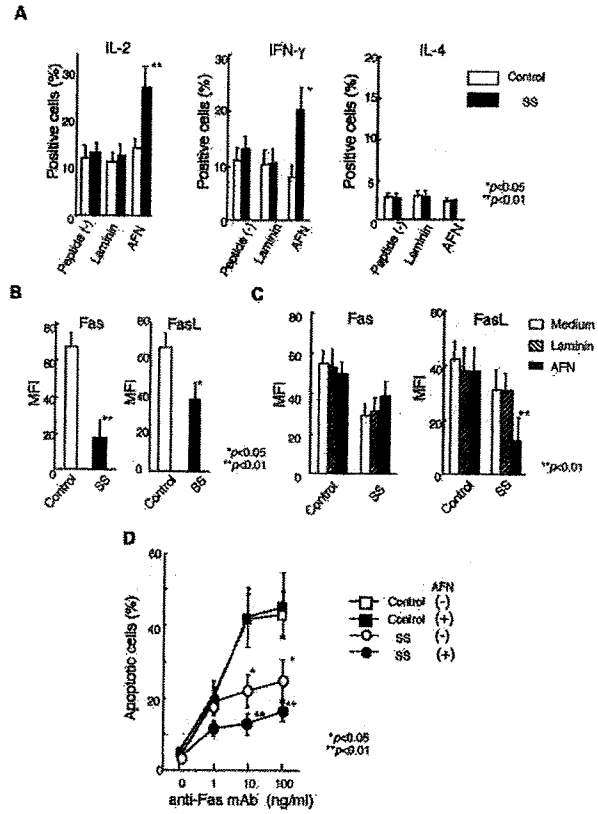

Figure 6. Cytokine profile and Fas-mediated apoptosis in $CD4^+$ T cells from SS patients. **A:** $CD4^+$ T cells from PBMCs with SS patients induce Th1 cytokine (IL-2, IFN-γ), not Th2 cytokine (IL-4) when pulsed with AFN peptide (10 μg/ml) by flow cytometric analysis ($^*P < 0.05$, $^{**}P < 0.01$; Student's *t*-test). Laminin fragment peptide 929-933 (10 μg/ml) was used as control. Five SS patients were analyzed. **B:** Significant decrease in both Fas^+ and $FasL^+$ expression in $CD4^+$ T cells from SS patients, compared with healthy controls ($^*P < 0.05$, $^{**}P < 0.01$; Student's *t*-test). Five SS patients and four healthy controls were analyzed. **C:** AFN peptide-pulsed $CD4^+$ T cells showing significant low intensity of FasL expression, not Fas expression, in SS patients ($^{**}P < 0.01$, Student's *t*-test). MFI (mean fluorescence intensity) indicates the fluorescence intensity of positively stained sample/the fluorescence intensity of its isotype control. Mean fluorescence intensity was calculated using the fluorescence intensity of staining for mAbs to Fas or FasL and isotype-matched control measured by flow cytometry. Five SS patients and four healthy controls were analyzed. **D:** Anti-Fas mAb-stimulated apoptosis showed significant decrease in $CD4^+$ T cells from SS patients than those from healthy control. Moreover, anti-Fas mAb-stimulated apoptosis decreased more significantly in $CD4^+$ T cells from SS patients pulsed with AFN peptide, than those with nonpulsed cells ($^*P < 0.05$, $^{**}P < 0.01$; Student's *t*-test). Five SS patients and four healthy controls were analyzed.

compared with healthy controls (Figure 6B). Moreover, it was demonstrated that AFN peptide-pulsed $CD4^+$ T cells showed a significant low intensity of FasL expression, not Fas expression (Figure 6C). Anti-Fas mAb-stimulated apoptosis showed a significant decrease in $CD4^+$ T cells from SS patients than those from healthy control (Figure 6D). When pulsed with AFN peptide, anti-Fas mAb-stimulated apoptosis decreased more significantly in $CD4^+$ T cells from SS patients.

Discussion

Cleavage of certain autoantigens during apoptosis may reveal immunocryptic epitopes that could potentially induce autoimmune responses in systemic autoimmune diseases.[26,27] We reported previously that a cleavage product of 120-kd α-fodrin may be an important autoantigen on the development of primary SS, and anti-120-kd α-fodrin antibodies have been frequently detected in sera from patients.[9] Although several candidate autoantigens besides α-fodrin have

been reported in SS,[28–30] the pathogenic roles of the autoantigens in initiation and progression of SS are still unclear.

The specificity of cytotoxic T-lymphocyte function has been an important issue of organ-specific autoimmune response, but little is known about the events triggering T-cell invasion of the target organs in prelude to organ-specific autoimmune diseases. In insulin-dependent diabetes mellitus, the role of environmental factors,[31,32] the nature of the initiating T cell,[33,34] and the identity of the inciting antigen(s)[35] have all been vigorously debated. When we analyzed the mechanisms of α-fodrin cleavage in the SS salivary glands, infiltrating mononuclear cells bear a large proportion of $CD4^+$ and Fas ligand (FasL), and the salivary gland duct cells constitutively possess Fas. In particular, cleavage products of 120-kd α-fodrin were frequently detected in the salivary gland duct cells with SS, but not in control salivary glands. Thus, we provided evidence suggesting that Fas-mediated apoptosis may be involved, in part, in *in vivo* α-fodrin cleavage in SS salivary glands. Moreover, it has been suggested that α-fodrin cleavage triggered by estrogen deficiency plays an important role in the development of autoimmune exocrinopathy in SS. Experimental studies of ours demonstrated a significant apoptosis associated with α-fodrin cleavage in the salivary gland cells of estrogen-deficient healthy C56BL/6(B6) mice, and inflammatory lesions developed exclusively in the salivary and lacrimal gland after the adoptive transfer with α-fodrin-reactive T cells in both ovariectomized (Ovx)-B6 and Ovx-SCID mice.[36] Reduction of the intact form of α-fodrin in the affected glands suggests that elicitation of autoreactivity against α-fodrin could be the primary pathogenetic process that leads to tissue destruction. However, based on the fact that α-fodrin is a ubiquitous protein, and that the tissue destruction is confined to exocrine organs, it might be more reasonable to speculate that other undetermined tissue-specific target antigens in exocrine glands could be the primary target of the disease process mediated by pathogenic T cells. Nevertheless, production of autoantibodies and proliferative T-cell responses against cleavage product of α-fodrin, which does not take place under physiological conditions, might be an important clue that could shed light on the novel mechanisms by which tissue-specific apoptosis contributes to the disease development.

It has been reported that calpain is overactivated in autoimmune conditions, and subsequent tissue destruction.[37,38] Moreover, the cascade of caspases is a critical component of the cell death pathway,[39–41] and a few proteins have been found to be cleaved during apoptosis. These include poly (ADP-ribose) polymerase, a small U1 nuclear ribonucleoprotein, and α-fodrin, which were subsequently identified as substrates for caspases.[27,42] Anti-Fas-induced cleavage of α-fodrin in Jurkat cells produces a predominant 120-kd fragment, and the 120-kd fragment is consistent with a previously reported caspase 3-mediated DETD cleavage site within the protein.[20,21] Although the relevance of cleavage of structural proteins, including gelsolin, actins, lamins, and fodrins, is easily conceivable,[43] the functional importance is not yet clear. Our data provide evidence that α-fodrin in human HSY cells is cleaved into 120-kd fragment by apoptotic proteases including calpain and caspases. When we investigated whether cysteine proteases are involved in α-fodrin cleavage, anti-Fas-treated HSY cells were positive for mAb to μ-calpain, and caspase 3 in association with apoptosis. However, we demonstrated here that calpastatin, an endogenous inhibitor of calpain, was shown to be constitutively expressed, speculating that μ-calpain activity could be considerably affected during apoptosis in HSY cells. A combination of calpain inhibitor peptide and caspase inhibitors (Z-VAD-fmk) entirely blocked the formation of 120-kd α-fodrin. When both full-length caspase 3 and μ-calpain cDNAs were transiently overexpressed in HSY cells, a cleavage product of 120-kd α-fodrin was abundantly identified than the level of expression of caspase 3 or μ-calpain in cells transfected with each construct. These data suggest that both μ-calpain and caspase 3 are required for specific α-fodrin proteolysis into the 120-kd fragment in human salivary gland cells with SS.

In this study, we detected proliferative T-cell responses to AFN protein (JS-1) of SS patients with short duration (within 5 years) from the onset of the disease were significantly higher than those with long duration (more than 5 years). Proliferative responses to autoantigen with younger SS patients (40 to 50 years of age) were significantly higher than those with older SS patients (60 to 70 years of age). Moreover, significant proliferative responses to AFN protein were observed in SS patients with higher pathological score (grade 4) than those with lower score (grade 2 or grade 3). These data are suggestive of clinicopathological usefulness of AFN immunoreactivity with SS patients for disease severity in addition to diagnostic significance. Because we have detected proliferative response to AFN peptides using PBMCs from SS patients, it is feasible for the future possibility that a peptide analogue of AFN could be used as a therapeutic agent. On the other hand, Fas/FasL interaction down-regulates the immune response by inducing apoptosis because activated lymphocytes express both Fas and FasL.[44] $CD4^+$ T cells from PBMCs with SS patients induce Th1 cytokine (IL-2, IFN-γ) when pulsed with each peptide, suggesting that the autoantigen peptide may play an important role in Th1/Th2 balance *in vivo*. Moreover, AFN peptide-pulsed $CD4^+$ T cells down-regulate Fas-mediated apoptosis. Although antigen-induced T-cell death is known to be regulated by CD4 expression,[45] molecular mechanisms responsible for T-cell death should be further elucidated. Our previous findings support the notion that Fas-mediated T-cell death is down-regulated by autoantigen stimulation in the murine SS model.[46] Here we demonstrated that AFN peptide stimulation results in a significant decrease in anti-Fas-induced $CD4^+$ T-cell apoptosis. However, it remains unclear whether T cells specific for endogenous

epitopes play a significant pathological role in tissue damage during the clinical episodes.

Taken together, our results suggest that 120-kd α-fodrin, the apoptosis-associated breakdown product, may have an important role in the development of SS, and that the autoantigen is a novel participant in the regulation of Th1/Th2 balance and peripheral tolerance.

References

1. Gianani R, Satventnick N: Virus, cytokine, antigens, and autoimmunity. Proc Natl Acad Sci USA 1996, 93:2257–2259
2. Feldmann M, Bennan FM, Maini RN: Rheumatoid arthritis. Cell 1996, 85:307–310
3. Fox RI, Robinson CA, Curd JG, Kozin F, Howell FV: Sjögren's syndrome. Proposed criteria for classification. Arthritis Rheum 1986, 29:577–585
4. Chan EK, Hamel JC, Buyon JP, Tan ET: Molecular definition and sequence motifs of the 52-kD component of human SS-A/Ro autoantigen. J Clin Invest 1991, 87:68–76
5. Kruize AA, Smeenk RJT, Kater L: Diagnostic criteria and immunopathogenesis of Sjögren's syndrome. Immunol Today 1995, 16:557–559
6. Fox RI, Stern M, Michelson P: Update in Sjögren's syndrome. Curr Opin Rheumatol 2000, 12:391–398
7. Manoussakis MN, Moutsopoulos HM: Sjögren's syndrome: current concepts. Adv Intern Med 2001, 47:191–217
8. Humpherys-Beher MG, Peck AB, Dang H, Talal N: The role of apoptosis in the initiation of the autoimmune response in Sjögren's syndrome. Clin Exp Immunol 1999, 116:383–387
9. Haneji N, Nakamura T, Takio K, Yanagi K, Higashiyama H, Saito I, Noji S, Sugino H, Hayashi Y: Identification of α-fodrin as a candidate autoantigen in primary Sjögren's syndrome. Science 1997, 276:604–607
10. Harrington CJ, Paez A, Hunkapiller T, Mannikko V, Brabb T, Ahearn M, Beeson C, Goverman J: Differential tolerance is induced in T cells recognizing distinct epitopes of myelin basic protein. Immunity 1998, 8:571–580
11. Dai Y, Carayanniotis KA, Eliades P, Lymberi P, Shepherd P, Kong Y, Carayanniotis G: Enhancing or suppressive effects of antibodies on processing of a pathogenic T cell epitope in thyroglobulin. J Immunol 1999, 162:6987–6992
12. Hoglund P, Mintern J, Waltzinger C, Heath W, Benoist C, Mathis D: Initiation of autoimmune diabetes by developmentally regulated presentation of islet cell antigens in the pancreatic lymph nodes. J Exp Med 1999, 189:331–339
13. Leto TL, Pleasic S, Forget BG, Benz Jr EJ, Marchesi VT: Characterization of the calmodulin-binding site of nonerythroid α-spectrin. J Biol Chem 1989, 264:5826–5830
14. Alnemri ES, Livingstin DJ, Nicholson DW, Salvensen G, Thornberry NA, Wong WW, Yuan J: Human ICE/CED-3 protease nomenclature. Cell 1996, 87:171
15. Martin SD, O'Brien GA, Nishioka WK, McGahon AJ, Mahboubi A, Saido TV, Green DR: Proteolysis of fodrin (non-erythroid spectrin) during apoptosis. J Biol Chem 1995, 270:6425–6428
16. Martin SD, Finucane DM, Amarante-Mendes GP, O'Brien GA, Green DR: Phosphatidylserine externalization during CD95-induced apoptosis of cells and cytoplasts requires ICE/CED-3 protease activity. J Biol Chem 1996, 271:28753–28756
17. Vanags DM, Pörn-Ares I, Coppolaa S, Burgess DH, Orrenius S: Protease involvement in fodrin cleavage and phosphatidylserine exposure in apoptosis. J Biol Chem 1996, 271:31075–31085
18. Nath R, Raser KJ, Stafford D, Hajimohammadreza I, Posner A, Allen H, Talanian RV, Yuen P, Gilbertsen RB, Wang KK: Non-erythroid α-spectrin breakdown by calpain and interleukin 1β-converting-enzyme-like protease(s) in apoptotic cells: contributory roles of both protease families in neuronal apoptosis. Biochem J 1996, 319:683–690
19. Janicke RU, Sprengart ML, Porter AG: Caspase-3 is required for alpha-fodrin cleavage but dispensable for cleavage of other death substrates in apoptosis. J Biol Chem 1996, 273:15540–15545
20. Cryns VL, Bergeron L, Zhu H, Li H, Yuan J: Specific cleavage of alpha-fodrin during Fas- and tumor necrosis factor-induced apoptosis is mediated by an interleukin-1beta-converting enzyme/Ced-3 protease distinct from the poly(ADP-ribose) polymerase protease. J Biol Chem 1996, 271:31277–31282
21. Wang KW, Posmantur R, Nath R, McGinnis K, Whitton M, Talanian RV, Glantz, Marrow JS: Simultaneous degradation of alphaII- and betaII-spectrin by caspase 3 (CPP32) in apoptotic cells. J Biol Chem 1998, 273:22490–22497
22. Tan EM, Cohen AS, Fries JF, Masi AT, McShane DJ, Rothfield NF, Schaller JG, Talal N, Winchester RJ: The 1982 revised criteria for the classification of systemic lupus erythematosus. Arthritis Rheum 1982, 25:1271–1277
23. Arnett FC, Edworthy SM, Bloch DA, McShane DJ, Fries JF, Cooper NS, Healey LA, Kaplan SR, Liang MH, Luthra HS: The American Rheumatism Association 1987 revised criteria for the classification of rheumatoid arthritis. Arthritis Rheum 1988, 31:315–324
24. Hayashi Y, Yanagawa T, Yoshida H, Azuma M, Nishida T, Yura Y, Sato M: Expression of vasoactive intestinal polypeptide and amylase in a human parotid gland adenocarcinoma cell line in culture. J Natl Cancer Inst 1987, 79:1025–1037
25. Enari M, Talanian RV, Wong WW, Nagata S: Sequential activation of ICE-like and CPP32-like proteases during Fas-mediated apoptosis. Nature 1996, 380:723–726
26. Utz PJ, Hottelet M, Schur PH, Anderson P: Proteins phosphorylated during stress-induced apoptosis are common targets for autoantibody production in patients with systemic lupus erythematosus. J Exp Med 1997, 185:843–854
27. Casiano CA, Martin SJ, Green DR, Tan EM: Selective cleavage of nuclear autoantigens ensuring CD95 (Fas/APO-1)-mediated T cell apoptosis. J Exp Med 1996, 184:765–770
28. Robinson CP, Brayer J, Yamachika S, Esch TR, Peck AB, Stewart CA, Peen R, Jonsson R, Humphreys-Beher MG: Transfer of human serum IgG to nonobese diabetic $Ig\mu^{null}$ mice reveals a role for autoantibodies in the loss of secretory function of exocrine tissues in Sjögren's syndrome. Proc Natl Acad Sci USA 1998, 95:7538–7543
29. Kuwana M, Okano T, Ogawa Y, Kaburaki J, Kawakami Y: Autoantibodies to the amino terminal fragment of β-fodrin expressed in glandular epithelial cells in patients with Sjögren's syndrome. J Immunol 2001, 167:5449–5456
30. Winer S, Astsaturov I, Cheung R, Tsui H, Song A, Gaedigk R, Winer D, Sampson A, McKerlie C, Bookman A, Dosch HM: Primary Sjögren's syndrome and deficiency of ICA69. Lancet 2002, 360:1063–1069
31. Singh B, Prange S, Jevnikar AM: Protective and destructive effects of microbial infection in insulin-dependent diabetes mellitus. Semin Immunol 1998, 10:79–86
32. Wong FS, Janeway Jr CA: The role of CD4 and CD8 T cells in type I diabetes in the NOD mouse. Res Immunol 1997, 148:327–332
33. Wegmann DR: The immune response to islets in experimental diabetes and insulin-dependent diabetes mellitus. Curr Opin Immunol 1996, 8:860–864
34. Kay TW, Chaplin HL, Parker JL, Stephens LA, Thomas HE: $CD4^+$ and $CD8^+$ T lymphocytes: clarification of their pathogenic roles in diabetes in the NOD mouse. Res Immunol 1997, 148:320–327
35. Patel T, Gores GJ, Kaufmann SH: The role of proteases during apoptosis. FASEB J 1996, 10:587–597
36. Ishimaru N, Arakaki R, Watanabe M, Kobayashi M, Miyazaki K, Hayashi Y: Development of autoimmune exocrinopathy resembling Sjogren's syndrome in estrogen-deficient mice of healthy background. Am J Pathol 2003, 163:1481–1490
37. Menad H-A, el-Amine M: The calpain-calpastatin system in rheumatoid arthritis. Immunol Today 1996, 17:545–547
38. Mimori T, Suganuma K, Tanami Y, Nojima T, Matsumura M, Fujii T, Yoshizaka T, Suzuki K, Akizuki M: Autoantibodies to calpastatin (an endogenous inhibitor for calcium-dependent neutral protease, calpain) in systemic rheumatic diseases. Proc Natl Acad Sci USA 1995, 92:7267–7271
39. Holtzman DM, Deshmukh M: Caspases: a treatment target for neurodegenerative disease? Nat Med 1997, 3:954–955
40. Rudel T, Bokoch GM: Membrane and morphological changes in

apoptotic cells regulated by caspase-mediated activation of PAK2. Science 1997, 276:1571–1574
41. Huang S, Jiang Y, Li Z, Nishida N, Mathias P, Lin S, Ulvitch RI, Nemerow GR, Han J: Apoptosis signaling pathway in T cells is composed of ICE/Ced-3 family proteases and MAP kinase kinase 6b. Immunity 1997, 6:739–749
42. Kothakota S, Azuma T, Reinhard C, Klippel A, Tang J, Chu K, McGarry TJ, Kirschner MW, Koths K, Kwiatkowski DJ, Williams LT: Caspase-3-generated fragment of gelsolin: effector of morphological change in apoptosis. Science 1997, 278:294–298
43. Feinstein E, Kimchi A, Wallach D, Boldin M, Varfolomeev E: The death domain: a module shared by proteins with diverse cellular function. Trends Biochem Sci 1995, 20:342–344
44. Van Parijs L, Ibraghimov A, Abbas AK: The roles of costimulation and Fas in T cell apoptosis and peripheral tolerance. Immunity 1996, 4:321–328
45. Hamad AR, Schneck JP: Antigen-induced T cell death is regulated by CD4 expression. Int Rev Immunol 2001, 20:535–546
46. Ishimaru N, Yanagi K, Ogawa K, Suda T, Saito I, Hayashi Y: Possible role of organ-specific autoantigen for Fas Ligand-mediated activation induced cell death in murine Sjögren's syndrome. J Immunol 2001, 167:6031–6037

Available online at www.sciencedirect.com

SCIENCE DIRECT

Autoimmunity Reviews 4 (2005) 479–484

AUTOIMMUNITY REVIEWS

www.elsevier.com/locate/autrev

The possible etiopathogenic genes of Sjögren's syndrome

Masami Takei[a,1], Hidetaka Shiraiwa[a,1], Takashi Azuma[b], Yoshio Hayashi[c], Naoyuki Seki[d], Shigemasa Sawada[a,e,*]

[a]*Department of Internal Medicine, Division of Hematology and Rheumatology, Nihon University, School of Medicine, Tokyo, Japan*
[b]*Department of Internal Medicine, Saitama Hospital, Saitama, Japan*
[c]*Department of Pathology, Tokushima University School of Dentistry, Tokushima, Japan*
[d]*Department of Clinical Molecular Biology, Graduate School of Medicine, Chiba University, Chiba, Japan*
[e]*Department of Medicine, Nerima Hikarigaoka Hospital, Nihon University School of Medicine, 2-11-1 Hikarigaoka Nerima-ku, Tokyo, Japan*

Received 17 April 2005; accepted 10 May 2005
Available online 31 May 2005

Abstract

Sjögren's syndrome is a chronic autoimmune disease characterized by focal lymphocytic infiltration of lacrimal and salivary glands, but the precise mechanism of this syndrome is unclear. To clarify the pathogenesis of Sjögren's syndrome, the related genes must be identified. In the present study, we investigate the increased expression of genes and molecules related to Sjögren's syndrome and present our findings of cDNA microarray analysis in the mouse model. Furthermore, we present the results of immunohistochemical analysis of salivary glands in the mouse model and patients with Sjögren's syndrome. This approach might open a new discussion of the existence of principal pathogenic molecules in Sjögren's syndrome.

Keywords: Sjögren's syndrome; MRL/lpr mice; NFS/sld mice; cDNA microarray; Human homologue of SS related genes

Contents

* Corresponding author. Department of Medicine, Nerima Hikarigaoka Hospital, Nihon University School of Medicine, 2-11-1 Hikarigaoka Nerima-Ku, Tokyo, Japan. Tel.: +81 3 3979 3611; fax: +81 3 3979 3868.
E-mail address: sswd98@med.nihon-u.ac.jp (S. Sawada).
[1] First two authors equally contributed.

1568-9972/$ - see front matter © 2005 Elsevier B.V. All rights reserved.
doi:10.1016/j.autrev.2005.05.003

1. Mouse model of Sjögren's syndrome

Sjögren's syndrome (SS) is an autoimmune disease characterized by the massive infiltration of lymphocytes into exocrine glands, such as salivary and lacrimal glands, and the subsequent destruction of these exocrine glands. Like other autoimmune diseases, the etiology of SS remains unclear, but previous studies suggest the involvement of hereditary and environmental factors in the onset and progression of the disease. The disease is usually benign and many patients live a typical lifespan. However, the most common symptoms, dry eyes and dry mouth, are problematic and deeply influence patients' quality of life. In addition to these relatively benign manifestations, abnormalities of more vital organs such as renal tubular acidosis, interstitial pulmonary fibrosis, and central nervous system involvement have been demonstrated [1–4]. Therefore, it is important to determine the etiology of SS for the improved management of the disease.

An animal model is one of the most useful tools for studying the pathogenesis of SS; several mouse models have been generated and extensively studied. Among these models, the MRL/lpr mouse bearing the *lpr* gene with a deletion of Fas antigen spontaneously develops systemic vasculitis, glomerulonephritis, arthritis, and sialoadenitis. High levels of autoantibodies, immune complexes, and rheumatoid factor have also been observed in this mouse model [5,6]. Inflammation of the salivary glands in the MRL/lpr mouse is widely accepted as a pathogenic model for human secondary SS [7]. Although the fundamental molecular abnormality in the MRL/lpr mouse model directly depends on the *lpr* gene, the extent of the phenotype and the timing of onset are strongly influenced by background genes [8–10].

The NFS/sld mutant mouse is an animal model of primary SS that bears an autosomal recessive gene that arrests sublingual gland differentiation. Autoimmune sialoadenitis develops when NFS/sld mice undergo a thymectomy 3 days after birth without any immunization (Tx-NFS/sld mice). While no significant inflammatory lesions are observed in other organs or in NFS/sld mice that do not undergo a thymectomy (non-Tx-NFS/sld mice), significant inflammatory changes occur in the salivary glands of Tx-NFS/sld mice 4 weeks after their thymectomy [11,12].

2. cDNA Microarray analysis

Gene expression analysis provides an important perspective on unknown biological phenomena. The following methods are established and applied for basic and clinical studies: differential display [13], suppression subtractive hybridization [14], cDNA microarray hybridization [15], and serial analysis of gene expression (SAGE) [16]. A microarray system is a powerful tool for analyzing the expression profile of thousands of genes in a wide range of biological systems. Recently, microarray analysis has been applied for the research of various clinical disorders such as lymphoma, Huntington's disease, and myocardial infarction, and disease-related genes were isolated in some of these disorders [17–21].

In the present study, we isolated genes that contribute to the progression of SS, using mRNA from SS model mouse salivary glands and an in-house cDNA microarray, and identified up-regulated genes.

3. Sjögren's syndrome-related genes and molecules

To investigate the gene expression profile in SS, we examined the mRNAs of the MRL/lpr and NFS/sld mouse salivary glands using cDNA microarrays. We arrayed a set of 4608 cDNA clones derived from oligo-capped mouse brain, fetus, kidney, and spleen. The most aggressive inflammation in the salivary gland of MRL/lpr mouse occurs at the age of 12–16 weeks [8,22], so we compared the mRNAs of MRL/lpr and MRL/++ mouse salivary glands at the age of 16 weeks. We identified 15 highly expressed genes [*IL-16*, *Grap*, *caspase3*, *Ly-6C.2*, *Mel-14 antigen*, *cathepsin B*, *mptl*, *Laptm5*, *Gnai2*, *vimentin*, *UCP2*, *saposin*, *Trt*, *laminin receptor 1*, *and HSP 70 cognate*] in the salivary gland of MRL/lpr mouse by cDNA microarray analysis, which were likely to be SS-related genes [23] (Table 1).

We performed reverse transcription-polymerase chain reaction amplification to confirm the high expression of the following 15 genes. High expression was verified in 11 of the 15 genes: *IL-16*, *Grap*, *caspase3*, *Ly-6C.2*, *vimentin*, *Mel-14 antigen*, *cathepsin B*, *mptl*, *Laptm5*, *Gnai2*, and *UCP2*. Five of these genes (*caspase 3*, *Ly-6C*, *vimentin*, *Mel-14 antigen*, and *cathepsin B*) have already been recognized in patients with SS or the SS mouse model [24–29].

Table 1
Highly expressed genes in MRL/lpr mice salivary gland in comparison with MRL/++

Accession No.	Name of genes	Fold change[a]
NM_009810	Mus musculus *caspase 3*	2.31
M18466	Mouse lymphocyte differentiation antigen *Ly-6C.2*	2.75
M26251	Mouse *vimentin*	2.21
M25324	Mouse peripheral lymph node-specific homing receptor (*MEL-14* antigen)	3.50
NM_007798	Mus musculus *cathepsin B*	1.84
AF006467	Mus musculus membrane-associated phosphatidylinositol transfer protein (*mpt1*)	1.98
NM_010686	Mus musculus lysosomal-associated protein transmembrane 5 (*Laptm5*)	2.16
NM_008138	Mus musculus guanine nucleotide binding protein, alpha inhibiting 2 (*Gnai2*)	1.93
U69135	Mus musculus *UCP2*	2.06
S36200	Mouse saposin=sphingolipid activator protein	1.88
NM_009429	Mus musculus translationally regurated transcript (*Trt*)	1.82
NM_011029	Mus musculus laminin receptor 1 (*Lamr1*)	2.02
M19141	Mouse heat shock protein 70 cognate	1.61
AF175292	Mus musculus neuronal *IL-16*	2.20
NM_027817	GRB2-related adaptor protein (*Grap*), mRNA	1.85

[a] The averages of the fold change based on the normalized microarray fluorescent data of MRL/lpr compared to MRL/++ ($n=8$).

Although a high expression of *caspase 3* has been reported in the NOD mouse model of SS [24], the MRL/lpr mouse is Fas-deficient and thus lacks Fas/Fas ligand pathway-dependent apoptosis. This suggests that Fas/Fas ligand pathway-independent apoptosis, such as perforin-or granzyme-dependent apoptosis [30], is induced in MRL/lpr mouse salivary glands. One of the adaptor molecules, Grap, effectively delivers signals from the immune cell surface to a downstream functional molecule. Grap has a structural arrangement of an SH3-SH2-SH3 domain, which is similar to that of other immune cell adaptor molecules such as Grb2, Gads, and Grap2 [31]. Grap is known to be specifically expressed in lymphoid tissues, and structurally resembles Grb2 more than other Grb2 family molecules in that Grap does not have the proline-rich motif. By immune cell activation, Grap binds to phosphorylated tyrosine of the local area transport (LAT) at its SH2 region, and further binds to Son of sevenless (Sos) in a manner similar to that of Grb2. Further down-stream events remain unknown. We have observed that the expression of Grap in the salivary glands of the model mice was higher than that of the control mice. Furthermore, we have identified 7 genes in the spleen of MRL/lpr mice not found in the spleen of MRL/+ mice using the mouse spleen cDNA microarray chip [32] (Table 2). Namely, the *Grap* gene was commonly up-regulated in the spleen and salivary glands from MRL/lpr mice [32]. Immunohistochemical staining in the salivary gland revealed substantial differences between MRL/lpr and MRL/++ in the expression of mouse Grap. Furthermore, the immunohistochemical staining of specimens from 3 patients with SS and 2 controls (subjects with salivary cysts) indicated that the human homologue of Grap was expressed on ductal cells and on certain infiltrating cells in patients with SS, but very weakly in the controls [32]. These results may suggest that in diseased salivary glands and spleen, enhanced stimulation of T cell receptor augments signal transduction to downstream molecules associated with apoptosis. Further detailed analysis of the Grb2 family may clarify the regulation of T cell differentiation and apoptosis in SS.

Table 2
Highly expressed genes in MRL/lpr mice spleen in comparison with MRL/++

Accession No.	Name of genes	Fold change[a]
U88682	Mouse anti-DNA antibody heavy chain variable region mRNA	2.88
XM_134565	Mouse similar to Gag-Pol polyprotein mRNA	1.93
M16072	Mouse Ig active gamma-2a H-chain V-Dsp2.2-J2-C mRNA	1.64
BC036286	Mouse myeloid/lymphoid or mixed-lineage leukemia 5, mRNA	2.17
NM_025408	Mouse phytoceramidase, alkaline (Phca)mRNA	3.23
X76772	Mouse mRNA for ribosomal protein S3	1.56
NM_027817	Mus musculus GRB2-related adaptor protein (*Grap*), mRNA	2.82

[a] The averages of the fold change based on the normalized microarray fluorescent data of MRL/lpr compared with MRL/+ ($n=6$).

To our knowledge, the remaining five genes (*mptl, Laptm5, UCP2 Gnai2* and *IL16*) have not been identified previously as SS-related genes. *Mptl* was cloned as a mouse homologue of Drosophila retinal degeneration B (rdgB), and the mptl protein has been predicted to be a membrane-bound phosphatidylinositol transfer protein (PITP) [33], which transports phosphatidylinositol (PI) through the aqueous phase from one membrane compartment to another and functions as a cofactor for the synthesis of phosphatidylinositol bisphosphate (PIP2) [34]. Given that the constitutive turnover of PI is markedly augmented in some subsets of T lymphocytes in MRL/lpr mice [35], it is fair to speculate that such T cells accumulate and are related to the pathogenesis of SS. *Laptm5* is highly expressed in adult hematopoietic organs such as bone marrow, spleen, thymus, lymph nodes, and peripheral blood leukocytes [36]. The high expression of *Laptm5* in our MRL/lpr mouse model of SS could be due to an increased number of lymphocytes infiltrating the salivary glands. Further experimental studies are required to clarify the role of *Laptm5* in the pathogenesis of SS. The mitochondrial protein known as uncoupling protein 2 (*UCP2*) is highly expressed in the spleen and macrophages. A recent report suggests that *UCP2* plays a role in limiting macrophage-mediated immunity [37]. The expression of *UCP2* is induced by TNF-α [38] and the expression of TNF-α is increased in MRL/lpr mice [39]. These combined findings suggest that increased TNF-α in MRL/lpr mouse salivary glands could contribute to the up-regulation of *UCP2* and subsequent disease progression.

We then examined the expression of these genes in the salivary glands of MRL/lpr mice and NFS/sld mice that had undergone a thymectomy (Tx-NFS/sld), a new model for primary SS, by using real-time-quantitative reverse transcription-polymerase chain reaction analysis. The expression of 11 genes (*IL-16*, *Grap*, *caspase3*, *Ly-6C.2*, *Mel-14 antigen*, *cathepsin B*, *mptl*, *Laptm5*, *Gnai2, vimentin,* and *UCP2)* was higher in MRL/lpr mice than in MRL/++ mice and the expression of 9 genes (*IL-16*, *Grap*, *caspase3*, *Ly6c2, Mel-14 antigen*, *cathepsinB*, *mptl Laptm5,* and *Gnai2)* was higher in the Tx-NFS/sld mice than in the control mice that did not undergo thymectomy. In addition, the fetus microarray analysis demonstrated that the *Laptm5* gene was also highly expressed in the salivary glands of Tx-NFS/sld mice. Furthermore, immunohistochemical studies showed that mouse and human *Laptm5* protein antigens were expressed on certain infiltrated lymphocytes and on ductal cells in the salivary glands from the SS mouse model and patients with SS, but very weakly in control subjects. These results suggest that some apoptosis-related genes might be responsible for the pathogenesis of organ-specific autoimmune lesions in SS (Arthritis Rheumatism Vol. 9, S251, 2001, Arthritis and Rheumatism Vol. 50 S577 2004).

These early findings confirm the excellent specificity and reproducibility of our cDNA microarray analysis for identification of disease-related genes. A microarray system can handle thousands of genes and help in the extraction of genes that have significant relationships to the stages of a disease. In addition, an in-house cDNA microarray is advantageous in allowing the exchange of arrayed genes and assaying specific disease-related genes on one glass slide, which is useful for the diagnosis and prediction of clinical stages.

In the present study, we isolated nine SS-related genes on a cDNA microarray using the MRL/lpr SS mouse model. Further studies may allow the identification of other SS-related genes, thus allowing the performance of clustering analysis, which could provide useful information about classification of the disease, clinical course, stage of the disease, and selection of a suitable treatment. The combination of an in-house microarray and the use of an animal model is a suitable strategy for exploring a gene expression profile and should gradually evolve into a system useful for clinical investigation.

Take-home message

- The combination of cDNA microarray and use of animal models is a suitable strategy for exploring a gene expression profile and should gradually evolve into a system useful for clinical investigation.
- Fifteen highly expressed genes, *IL-16*, *Grap*, *caspase3*, *Ly-6C.2*, *Mel-14 antigen*, *cathepsin B*, *mptl*, *Laptm5*, *Gnai2, vimentin*, *UCP2*, *saposin*, *Trt*, *laminin receptor 1*, and *HSP 70 cognate*, in the salivary gland of MRL/lpr mouse by cDNA microarray analysis were identified.
- The expression of 9 genes, *IL-16*, *Grap*, *caspase3*, *Ly6c2, Mel-14 antigen*, *cathepsin B*, *mptl Laptm5*, and *Gnai2,* was higher in the salivary gland of

thymectomized-NFS/sld mice than in the control mice that did not undergo thymectomy.

- Five genes, *mpt1, Laptm5, UCP2 Gnai2* and *IL16*, have not been identified previously as SS-related genes.
- Human *Grap* and *Laptm5* protein antigens were expressed on certain infiltrated lymphocytes and on ductal cells in the salivary glands from patients with SS, but very weakly in control subjects.

References

[1] Talal N, Sokoloff L, Barth WF. Extrasalivary lymphoid abnormalities in Sjögren's syndrome reticulum cell sarcoma, "pseudolymphoma", macroglobulinemia. Am J Med 1967; 43:50–65.

[2] Hoffman RW, Alspaugh MA, Waggle KS, Durham JB, Walker SE. Sjögren's syndrome in MRL/lpr and MRL/n mice. Arthritis Rheum 1984;27:157–65.

[3] Moutsopoulous HM, Fauci AS. Immunoregulation in Sjögren's syndrome: influence of serum factors on T-cell subpopulations. J Clin Invest 1980;65:519–28.

[4] Fox RI. Clinical feature, pathogenesis, and treatment of Sjögren's syndrome. Curr Opin Rheumatol 1996;8:438–45.

[5] Izui S, Kelley VE, Masuda K, Yoshida H, Roths JB, Murphy ED. Induction of various autoantibodies by mutant gene *lpr* in several strains of mice. J Immunol 1984;133: 227–33.

[6] Watanabe-Fukunaga R, Brannan CI, Copeland NG, Jenkins NA, Nagata S. Lymphoproliferation disorder in mice explained by defects in Fas antigen that mediates apoptosis. Nature 1992;356:314–7.

[7] Hayashi Y, Haneji N, Hamano H. Pathogenesis of Sjögren's syndrome-like autoimmune lesions in MRL/lpr mice. Pathol Int 1994;44:559–68.

[8] Jabs DA, Lee B, Whittum-Hudson J, Prendergast RA. The role of Fas–Fas ligand-mediated apoptosis in autoimmune lacrimal gland disease in MRL/MpJ mice. Invest Ophthalmol Vis Sci 2001;42:399–401.

[9] Cohen PL, Eisenberg RA. *Lpr* and *gld* single gene models of systemic autoimmunity and lymphoproliferative disease. Annu Rev Immunol 1991;9:243–69.

[10] Nakatsuru S, Terada M, Nishihara M, Kamogawa J, Miyazaki T, Qu WM, et al. Genetic dissection of the complex pathological manifestations of collagen disease in MRL/lpr mice. Pathol Int 1999;49:974–82.

[11] Haneji N, Hamano H, Yanagi K, Hayashi Y. A new animal model for primary Sjögren's syndrome in NFS/sld mutant mice. J Immunol 1994;153:2769–77.

[12] Hayashi Y, Haneji N, Hamano H, Yanagi K, Takahashi M, Ishimaru N. Effector mechanism of experimental autoimmune sialoadenitis in the mouse model for primary Sjögren's syndrome. Cell Immunol 1996;171:217–25.

[13] Liang P, Pardee AB. Differential display of eukaryotic messenger RNA by means of the polymerase chain reaction. Science 1992;257:967–71.

[14] Diatchenko L, Lau YF, Campbell AP, Chenchik A, Moqadam F, Huang B, et al. Suppression subtractive hybridization: a method for generating differentially regulated or tissue-specific cDNA probes and libraries. Proc Natl Acad Sci USA 1996;93:6025–30.

[15] Schena M, Shalon D, Davis RW, Brown PO. Quantitative monitoring of gene expression patterns with a complementary DNA microarray. Science 1995;270:467–70.

[16] Velculescu VE, Zhang L, Vogelstein B, Kinzler KW. Serial analysis of gene expression. Science 1995;270:484–7.

[17] Brown PO, Botstein D. Exploring the new world of the genome with DNA microarrays. Nat Genet 1999;21:33–7.

[18] Yoshikawa T, Nagasugi Y, Azuma T, Kato M, Sugano S, Hashimoto K, et al. Isolation of novel mouse genes differentially expressed in brain using cDNA microarray. Biochem Biophys Res Commun 2000;275:532–7.

[19] Alizadeh AA, Eisen MB, Davis RE, Ma C, Lossos IS, Rosenwald A, et al. Distinct types of diffuse large B-cell lymphoma identified by gene expression profiling. Nature 2000;403: 503–11.

[20] Luthi-Carter R, Strand A, Peters NL, Solano SM, Hollingsworth ZR, Menon AS, et al. Decreased expression of striatal signaling genes in a mouse model of Huntington's disease. Hum Mol Genet 2000;9:1259–71.

[21] Stanton LW, Garrard LJ, Damm D, Garrick BL, Lam A, Kapoun AM, et al. Altered patterns of gene expression in response to myocardial infarction. Circ Res 2000;86: 939–45.

[22] van Blokland SC, van Helden-Meeuwsen CG, Wierenga-Wolf AF, Drexhage HA, Hooijkaas H, van de Merwe JP, et al. Two different types of sialoadenitis in the NOD- and MRL/lpr mouse models for Sjögren's syndrome: a differential role for dendritic cells in the initiation of sialoadenitis? Lab Invest 2000;80:575–85.

[23] Azuma T, Takei M, Yoshikawa T, Nagasugi Y, Kato M, Shiraiwa H, et al. Identification of candidate genes for Sjogren's syndrome using MRL/lpr mouse model of Sjögren's syndrome and cDNA microarray analysis. Immunol Lett 2002;81:171–6.

[24] Robinson CP, Yamachika S, Alford CE, Cooper C, Pichardo EL, Shah N, et al. Elevated levels of cysteine protease activity in saliva and salivary glands of the nonobese diabetic (NOD) mouse model for Sjogren syndrome. Proc Natl Acad Sci USA 1997;94:5767–71.

[25] Dumont FJ. Stimulation of murine T cells via the Ly-6C antigen: lack of proliferative response in aberrant T cells from lpr/lpr and gld/gld mice despite high Ly-6C antigen expression. J Immunol 1987;138:4106–13.

[26] Andre-Schwartz J, Datta SK, Shoenfeld Y, Isenberg DA, Stollar BD, Schwartz RS. Binding of cytoskeletal proteins by monoclonal anti-DNA lupus autoantibodies. Clin Immunol Immunopathol 1984;31:261–71.

[27] Kjorell U, Ostberg Y. Distribution of intermediate filaments and actin microfilaments in parotid autoimmune sialoadenitis of Sjögren syndrome. Histopathology 1984;8:991–1011.

[28] Takahashi M, Mimura Y, Hayashi Y. Role of the ICAM-1/LFA-1 pathway during the development of autoimmune dacryoadenitis in an animal model for Sjögren's syndrome. Pathobiology 1996;64:269–74.
[29] Steinfeld S, Maho A, Chaboteaux C, Daelemans P, Pochet R, Appelboom T, et al. Prolactin up-regulates cathepsin B and D expression in minor salivary glands of patients with Sjögren's syndrome. Lab Invest 2000;80:1711–20.
[30] Fujihara T, Fujita H, Tsubota K, Saito K, Tsuzaka K, Abe T, et al. Preferential localization of CD8+ (E)7+ T cells around acinar epithelial cells with apoptosis in patients with Sjögren's syndrome. J Immunol 1999;163:2226–35.
[31] Liu SK, Berry DM, McGlade CJ. The role of Gads in hematopoietic cell signaling. Oncogene 2001;20:6284–90.
[32] Shiraiwa H, Takei M, Yoshikawa T, Azuma T, Kato M, Mitamura K, et al. Detection of Grb-2-related adaptor protein gene (GRAP) and peptide molecule in salivary glands of MRL/lpr mice and patients with Sjögren's syndrome. J Int Med Res 2004;32:284–91.
[33] Aikawa Y, Hara H, Watanabe T. Molecular cloning and characterization of mammalian homologues of the drosophila retinal degeneration Bgene. Biochem Biophys Res Commun 1997;236:559–64.
[34] Cockcroft S. Phosphatidylinositol transfer proteins: a requirement in signal transduction and vesicle traffic. Bioessays 1998;20:423–32.
[35] Tomita-Yamaguchi M, Santoro TJ. Constitutive turnover of inositol-containing phospholipids in B220+ T cells from autoimmune-prone MRL-lpr/lpr mice. J Immunol 1990;144:3946–52.
[36] Adra CN, Zhu S, Ko JL, Guillemot JC, Cuervo AM, Kobayashi H, et al. *LAPTM5*: A novel lysosomal-associated multispanning membrane protein preferentially expressed in hematopoietic cells. Genomics 1996;35:328–37.
[37] Arsenijevic D, Onuma H, Pecqueur C, Raimbault S, Manning BS, Miroux B, et al. Disruption of the uncoupling protein-2 gene in mice reveals a role in immunity and reactive oxygen species production. Nat Genet 2000;26:435–9.
[38] Masaki T, Yoshimatsu H, Chiba S, Hidaka S, Tajima D, Kakuma T, et al. Tumor necrosis factor—regulates in vivo expression of the rat UCP family differentially. Biochim Biophys Acta 1999;1436:585–92.
[39] Chan OT, Madaio MP, Shlomchik MJ. The central and multiple roles of B cells in lupus pathogenesis. Immunol Rev 1999;169:107–21.

Endometriosis and systemic lupus erythematosus: a comparative evaluation of clinical manifestations and serological autoimmune phenomena.

Due to evidences suggesting association between endometriosis (EM) and systemic lupus erythematosus (SLE), Pasoto SG. et al. (Am J Reprod Immunol 2005;53:85–93), have performed a comparative evaluation of clinical and humoral immunologic abnormalities in both diseases. Forty-five women with histologically confirmed pelvic EM, 21 healthy-women and 15 female SLE-patients without surgically confirmed EM were prospectively evaluated. None of the EM-patients fulfilled criteria for SLE. However, EM-patients presented higher frequencies of arthralgia (62%) and generalized myalgia (18%) compared to that of normal-controls (24%, $p = 0.04$) but comparable with SLE-patients. Antinuclear antibodies (ANA) were detected in 18% of EM-patients, as compared with healthy-women ($p = 0.01$). Anti-Ro and anticardiolipin antibodies were more often in SLE (40%, 33%) than in EM-patients (2%, $p < 0.001$ and 9% $p = 0.04$). Elevated immune-complexes and low total complement were also more frequent in SLE patients. The data indicate differences of ANA antigenic specificity and complement consumption between EM and SLE. The high prevalence of generalized musculoskeletal complaints in EM justifies a multidisciplinary approach.

Two cases of antinuclear antibody negative lupus showing increased proportion of B cells lacking RP105.

B cells lacking RP105 molecule, a member of the Toll-like receptor family, were increased in the peripheral blood of 2 patients with antinuclear antibody (ANA) negative systemic lupus erythematosus (SLE). The increased proportion of RP105-lacking B cells was associated with disease activity in patients with ANA-negative SLE. Koarada S. et al (J Rheumatol 2005; 32:562-4) suggested that when there are no significant serological markers for SLE, analyses of expression of RP105 may be helpful in evaluation of activity in ANA-negative SLE. Thus they describe a new approach, using phenotyping of B cells, to evaluate activity of ANA-negative SLE.

nature genetics

Mutations in the gene encoding fibroblast growth factor 10 are associated with aplasia of lacrimal and salivary glands

Miriam Entesarian[1], Hans Matsson[1], Joakim Klar[1], Birgitta Bergendal[2], Lena Olson[3], Rieko Arakaki[4], Yoshio Hayashi[4], Hideyo Ohuchi[5], Babak Falahat[6], Anne Isine Bolstad[7], Roland Jonsson[8], Marie Wahren-Herlenius[9] & Niklas Dahl[1]

Autosomal dominant aplasia of lacrimal and salivary glands (ALSG; OMIM 180920 and OMIM 103420) is a rare condition characterized by irritable eyes and dryness of the mouth. We mapped ALSG to 5p13.2–5q13.1, which coincides with the gene fibroblast growth factor 10 (*FGF10*). In two extended pedigrees, we identified heterozygous mutations in *FGF10* in all individuals with ALSG. *Fgf10*$^{+/-}$ mice have a phenotype similar to ALSG, providing a model for this disorder. We suggest that haploinsufficiency for FGF10 during a crucial stage of development results in ALSG.

ALSG has variable expressivity, and affected individuals may have aplasia or hypoplasia of the lacrimal, parotid, submandibular and sublingual glands and absence of the lacrimal puncta[1]. The disorder is characterized by irritable eyes, recurrent eye infections, epiphora (constant tearing) and xerostomia (dryness of the mouth), which increases the risk of dental erosion, dental caries, periodontal disease and oral infections[2]. Individuals affected with ALSG are sometimes misdiagnosed with the more prevalent disorder Sjögren syndrome, an autoimmune disorder characterized by keratoconjunctivitis sicca and xerostomia[3]. Both sporadic and familial cases of ALSG have been described[2,4,5]. We recently identified two extended families of Swedish origin with ALSG (**Fig. 1a**). The phenotypes of the affected individuals are summarized in **Supplementary Table 1** online. In total, 16 individuals from both families were diagnosed with ALSG (**Supplementary Methods** online). We investigated the lacrimal and major salivary glands by magnetic resonance imaging (**Supplementary Fig. 1** online), which showed aplasia or hypoplasia of several major salivary glands in all affected individuals and absent or hypoplastic lacrimal glands in 13 of 14 affected individuals. We observed absence of one or several lacrimal puncta in 13 of 14 affected individuals. We observed no other abnormalities, and the affected individuals had normal lifespans.

Inheritance of ALSG in both families is autosomal dominant, and the segregation pattern suggested full penetrance. A genome-wide screen with 400 polymorphic microsatellite markers showed linkage of ALSG to 5p13.2–5q13.1 flanked by microsatellite markers *D5S395* and *D5S2046* (**Fig. 1a**). We obtained a maximum cumulative lod score of 5.72 ($\theta = 0$) at the marker locus *D5S398* for both families (**Supplementary Table 2** online). The gene fibroblast growth factor 10 (*FGF10*) is located in the linked region[6]. Mouse FGF10, which is 93% identical to human FGF10, is crucial for the development of several organs, including lacrimal and salivary glands[7–9]. *Fgf10*$^{-/-}$ mice die shortly after birth[9,10]. No abnormalities have been described in *Fgf10*$^{+/-}$ mice.

We considered *FGF10* as a candidate gene for ALSG. Sequence analysis of the three exons of *FGF10* in samples from family 1 showed no alterations compared with sequences in the National Center for Biotechnology Information database. To identify deletions, we genotyped the family members for SNPs and microsatellite markers in *FGF10*. The affected members of family 1 were hemizygous with respect to two dinucleotide repeats (TA53 and CA17) and three SNPs (rs10060548, rs6881797 and rs2290070; **Fig. 1b,c**). After genotyping, we characterized the deletion breakpoint by long-range PCR and sequencing across the breakpoint (**Supplementary Fig. 2** online). We determined the size of the deletion to be 53 kb, including exons 2 and 3, without the involvement of any flanking genes (**Fig. 1b**). In family 2, DNA sequence analysis of *FGF10* identified a heterozygous stop mutation in exon 3 (R193X; 577C→T) resulting in a predicted truncated protein in the four affected members (**Fig. 1d**).

We then reexamined *Fgf10*$^{+/-}$ mice, which were previously described as apparently normal[8,10]. We dissected adult mice and carried out a macroscopical and histological examination of the lacrimal and salivary gland apparatuses. *Fgf10*$^{+/-}$ mice had aplasia of lacrimal glands and hypoplasia of salivary glands (**Fig. 2**). These findings are consistent with the phenotype of individuals with ALSG. Other internal organs, including lung, liver, spleen, heart, stomach, thyroid, pancreas, intestines and ovaries, were macroscopically normal in *Fgf10*$^{+/-}$ mice.

To clarify whether *FGF10* mutations cause dry eyes and dry mouth in sporadic cases with symptoms identical to those of individuals with ALSG, we screened DNA samples from 74 individuals for mutations in *FGF10*. These individuals had been evaluated and diagnosed with dry eyes and/or dry mouth, without fulfilling the criteria for Sjögren syndrome[11,12]. We found no sequence alterations in the coding region of *FGF10* in samples from these individuals,

[1]Department of Genetics and Pathology, Uppsala University, The Rudbeck laboratory, SE-751 85 Uppsala, Sweden. [2]National Oral Disability Centre and [3]Department of Pediatric Dentistry, The Institute for Postgraduate Dental Education, Box 1030, SE-551 11 Jönköping, Sweden. [4]Department of Oral Molecular Pathology, Institute of Health Bioscience, The University of Tokushima Graduate School and [5]Department of Biological Science and Technology, Faculty of Engineering, University of Tokushima, Tokushima 770-8506, Japan. [6]Department of Maxillofacial Radiology, The Institute for Postgraduate Dental Education, Box 1030, SE-551 11 Jönköping, Sweden. [7]Department of Odontology-Periodontics, Faculty of Dentistry, University of Bergen, Aarstedveien 17, N-5009 Bergen, Norway. [8]Broegelmann Research Laboratory, The Gade Institute, University of Bergen, Armauer Hansen Building, N-5021 Bergen, Norway. [9]Department of Medicine, Karolinska Institutet, SE-171 76 Stockholm, Sweden. Correspondence should be addressed to N.D. (niklas.dahl@genpat.uu.se).

Published online 16 January 2005; doi:10.1038/ng1507

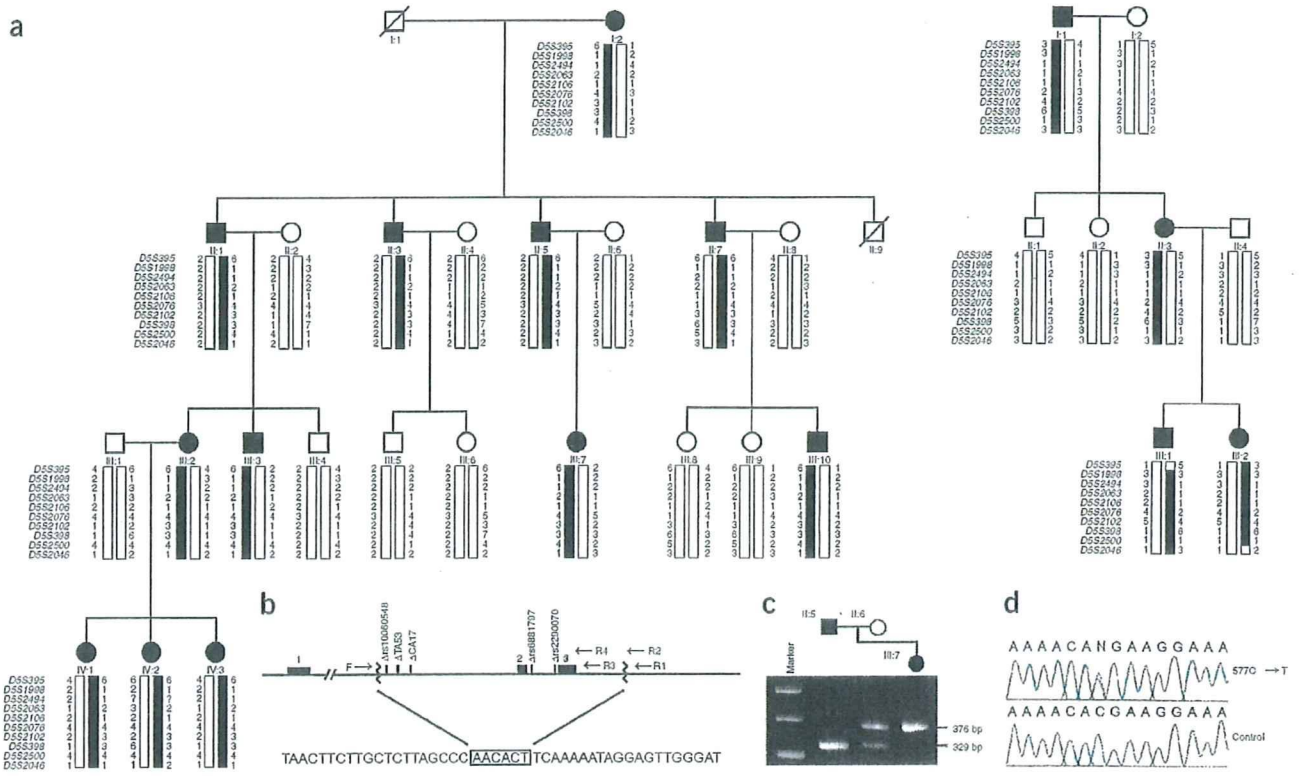

Figure 1 ALSG mapping. (**a**) Two pedigrees segregating for ALSG. Marker haplotypes on chromosome 5p13.2–5q13.1 that are linked to ALSG are indicated by black bars. (**b**) Schematic overview of *FGF10* and the 53-kb deletion inherited with ALSG in family 1 (figure not drawn to scale). Black boxes denote exons 1–3, and wavy vertical lines indicate deletion breakpoints. Genomic sequence spanning the breakpoint is shown. (**c**) Genotyping of the SNP rs6881797, located in the deletion found in family 1 and 37 bp 3′ of exon 2, by digestion with *BsrI*. Undigested PCR product (376 bp) corresponds to the T allele and digested PCR product (329 bp) corresponds to the A allele. The absence of a paternal A allele in individual III:7 in family 1 indicates hemizygosity with respect to rs6881797. (**d**) The upper sequence chromatogram illustrates the heterozygous (R193X; 577C→T) mutation found in the affected members of family 2. The lower sequence chromatogram illustrates the corresponding normal sequence.

suggesting that mutations in *FGF10* are uncommon in individuals with unspecific sicca syndromes.

In family 1, the affected individuals are hemizygous with respect to exons 2 and 3 of *FGF10*. In family 2, the premature stop codon (R193X; 577C→T) in exon 3 predicts a truncated protein with a loss of 16 amino acids. The truncation abolishes one predicted cAMP- and cGMP-dependent protein kinase phosphorylation site (residues 194–197) and one predicted *N*-linked glycosylation site (residues 196–198)[13]. Furthermore, the truncation eliminates one of the sites for the interaction between FGF10 and fibroblast growth factor receptor 2b (FGFR2b) at residues 202 and 204 (ref. 14). If produced, the truncated FGF10 is probably unstable or nonfunctional. Both mutations in *FGF10* that we identified are consistent with the idea that haploinsufficiency with respect to FGF10 underlies ALSG.

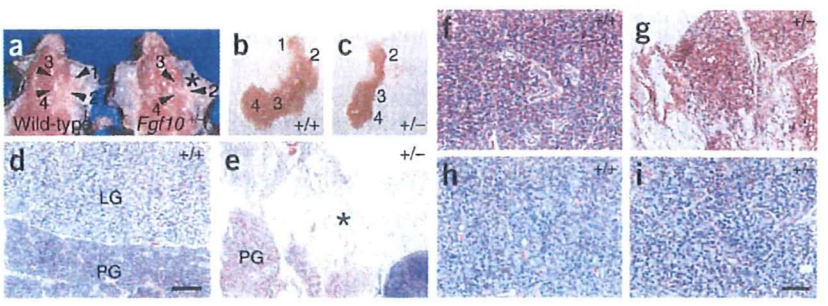

Figure 2 Salivary and lacrimal gland apparatuses of wild-type and *Fgf10*$^{+/-}$ mice. (**a**) Macroscopic examination of wild-type (left) and *Fgf10*$^{+/-}$ (right) adult mice. Ventral view of the mandibular region. 1, lacrimal; 2, parotid; 3, sublingual; 4, submandibular glands. The asterisk indicates the expected site for the lacrimal gland, which was absent in the heterozygote. Other glands were hypoplastic in the heterozygote. (**b**,**c**) Dissected salivary and lacrimal glands from the wild-type (**b**) and *Fgf10*$^{+/-}$ (**c**) mice. The salivary glands from the *Fgf10*$^{+/-}$ mouse were hypoplastic and the lacrimal gland was absent. (**d**–**i**) Histology of wild-type (**d**,**f**,**h**) and *Fgf10*$^{+/-}$ (**e**,**g**,**i**) glands. (**d**) Wild-type lacrimal (LG) and parotid (PG) glands. (**e**) The lacrimal gland was replaced by adipose tissue (asterisk) in the *Fgf10*$^{+/-}$ mouse. (**f**) Wild-type parotid gland. (**g**) Parotid gland from *Fgf10*$^{+/-}$ mouse, which appears atrophic. (**h**,**i**) Submandibular glands have similar histology in the wild type and heterozygote, as did sublingual glands (not shown). Scale bars: **d** (for panels **d** and **e**), 0.5 mm; **i** (for panels **f**–**i**), 0.1 mm.

The clinical examinations and medical histories of the affected family members illustrate that one intact copy of *FGF10* is sufficient for development of essential organs in humans. The restricted phenotype associated with heterozygosity with respect to *FGF10* in both humans and mice suggests that the response to FGF10 is dosage-sensitive. This is probably related to a specific embryonic stage and occurs at the site of lacrimal and salivary gland formation. A possible explanation for the absence of generalized effects in *FGF10* hemizygotes is a functional overlap with other FGFR2b ligands, such as FGF1, FGF3 and FGF7 (ref. 15).

The identification of mutations in *FGF10* as causing ALSG will hopefully result in increased diagnostic accuracy. In a larger context, this report clarifies the phenotypic effects of mutations in *FGF10* and may lead to a better understanding of the mechanisms involved in lacrimal and salivary gland formation.

We obtained informed consent from all participants in the study under a protocol approved by the Ethical Committee at Uppsala University or by the collaborating Universities.

URLs. Primer 3 is available at http://www-genome.wi.mit.edu/cgi-bin/primer/primer3_www.cgi/. The National Center for Biotechnology Information Entrez Genome Map Viewer is available at http://www.ncbi.nlm.nih.gov/mapview. The Ensembl Human Genome Server database is available at http://www.ensembl.org/. The Genome Database is available at http://www.gdb.org/.

Accession numbers. GenBank: human *FGF10*, NM_004465; human chromosome 5 clones containing *FGF10*, AC093537.2 and AC093289.2. GenBank Protein: human FGF10, NP_004456.1.

Note: Supplementary information is available on the Nature Genetics website.

ACKNOWLEDGMENTS

We thank the family members that participated in this study, N. Hagwall and M. Wyon for ophthalmologic examinations and L. Cato and Uppsala Genome Center. This work was supported by grants to N.D. from the Swedish Research Council, Swedish Cancer Society, Childrens' Cancer Foundation of Sweden, the Torsten and Ragnar Söderbergs Fund, the Borgström Foundation and Uppsala University.

COMPETING INTERESTS STATEMENT

The authors declare that they have no competing financial interests.

Received 24 August; accepted 22 December 2004
Published online at http://www.nature.com/naturegenetics/

1. Wiedemann, H.R. *Am. J. Med. Genet.* **68**, 222–224 (1997).
2. Ferreira, A.P. *et al. Am. J. Med. Genet.* **94**, 32–34 (2000).
3. Bolstad, A.I. & Jonsson, R. *Arthritis Res.* **4**, 353–359 (2002).
4. Young, W. *et al. Oral Surg. Oral Med. Oral Pathol. Oral Radiol. Endod.* **92**, 38–48 (2001).
5. Milunsky, J.M., Lee, V.W., Siegel, B.S. & Milunsky, A. *Am. J. Med. Genet.* **37**, 371–374 (1990).
6. Emoto, H. *et al. J. Biol. Chem.* **272**, 23191–23194 (1997).
7. Makarenkova, H.P. *et al. Development* **127**, 2563–2572 (2000).
8. Ohuchi, H. *et al. Biochem. Biophys. Res. Commun.* **277**, 643–649 (2000).
9. Min, H. *et al. Genes Dev.* **12**, 3156–3161 (1998).
10. Sekine, K. *et al. Nat. Genet.* **21**, 138–141 (1999).
11. Vitali, C. *et al. Arthritis Rheum.* **36**, 340–347 (1993).
12. Vitali, C. *et al. Ann. Rheum. Dis.* **61**, 554–558 (2002).
13. Bagai, S. *et al. J. Biol. Chem.* **277**, 23828–23837 (2002).
14. Yeh, B.K. *et al. Proc. Natl. Acad. Sci. USA* **100**, 2266–2271 (2003).
15. De Moerlooze, L. *et al. Development* **127**, 483–492 (2000).

Development of Autoimmunity against Transcriptionally Unrepressed Target Antigen in the Thymus of Aire-Deficient Mice[1]

Noriyuki Kuroda,* Tasuku Mitani,* Naoki Takeda,† Naozumi Ishimaru,‡ Rieko Arakaki,‡ Yoshio Hayashi,‡ Yoshimi Bando,§ Keisuke Izumi,§ Takeshi Takahashi,¶ Takashi Nomura,¶ Shimon Sakaguchi,¶‖ Tomoo Ueno,# Yousuke Takahama,# Daisuke Uchida,* Shijie Sun,* Fumiko Kajiura,* Yasuhiro Mouri,* Hongwei Han,* Akemi Matsushima,* Gen Yamada,† and Mitsuru Matsumoto[2]*

Autoimmune regulator (AIRE) gene mutation is responsible for the development of organ-specific autoimmune disease with monogenic autosomal recessive inheritance. Although Aire has been considered to regulate the elimination of autoreactive T cells through transcriptional control of tissue-specific Ags in thymic epithelial cells, other mechanisms of AIRE-dependent tolerance remain to be investigated. We have established Aire-deficient mice and examined the mechanisms underlying the breakdown of self-tolerance. The production and/or function of immunoregulatory T cells were retained in the Aire-deficient mice. The mice developed Sjögren's syndrome-like pathologic changes in the exocrine organs, and this was associated with autoimmunity against a ubiquitous protein, α-fodrin. Remarkably, transcriptional expression of α-fodrin was retained in the Aire-deficient thymus. These results suggest that Aire regulates the survival of autoreactive T cells beyond transcriptional control of self-protein expression in the thymus, at least against this ubiquitous protein. Rather, Aire may regulate the processing and/or presentation of self-proteins so that the maturing T cells can recognize the self-Ags in a form capable of efficiently triggering autoreactive T cells. With the use of inbred Aire-deficient mouse strains, we also demonstrate the presence of some additional factor(s) that determine the target-organ specificity of the autoimmune disease caused by Aire deficiency. *The Journal of Immunology,* **2005, 174: 1862–1870.**

Autoimmune diseases are mediated by sustained adaptive immune responses specific for self-Ags through unknown mechanisms. Although breakdown of self-tolerance is considered to be the key event in the disease process, the mechanisms that allow the production of auto-Abs and/or autoreactive lymphocytes are largely enigmatic (1). The situation seems to have become more complicated due to the existence of multiple factors that influence the disease process, such as environmental factors, immune dysregulation, and genetic predisposition. In this regard, although only a small number of genes genetically relevant to the pathogenetic processes for the development of autoimmune diseases have been found so far (2), genetic engineering of such genes in mice should enable us to establish disease models and facilitate an understanding of the disease mechanisms to a large extent. One of these genes is the autoimmune regulator (*AIRE*)[3] mutation, which is responsible for the development of autoimmune-polyendocrinopathy-candidiasis ectodermal dystrophy (APECED; Online Mendelian Inheritance in Man 240300) with autosomal recessive inheritance (3–6).

The *AIRE* gene encodes a predicted 58-kDa protein carrying a conserved nuclear localization signal, two plant homeodomain (PHD)-type zinc fingers, four LXXLL motifs or nuclear receptor interaction domains, and the recently described homogeneously staining region (HSR) and SAND domains (3, 4); the HSR and SAND domains have been suggested to function in homodimerization and DNA binding, respectively (7, 8). Based on the fact that PHD resembles the RING finger, which can function as an E3 ubiquitin ligase, in both sequence and structure (9), we have recently found that AIRE acts as an E3 ubiquitin ligase through the N-terminal PHD domain (PHD1) (10). Because the ubiquitin-proteasome pathway plays an essential role in diverse cell functions such as cell cycle progression, signal transduction, cell differentiation, DNA repair and apoptosis (11, 12), we speculate that AIRE should play a fundamental role by facilitating polyubiquitinylation of the substrate(s) in yet undetermined processes. The significance

*Division of Molecular Immunology, Institute for Enzyme Research, University of Tokushima, Tokushima, Japan; †Center for Animal Resources and Development, and Graduate School of Molecular and Genomic Pharmacy, Kumamoto University, Kumamoto, Japan; ‡Department of Pathology, Tokushima University School of Dentistry, Tokushima, Japan; §Department of Molecular and Environmental Pathology, School of Medicine, University of Tokushima, Tokushima, Japan; ¶Department of Experimental Pathology, Institute for Frontier Medical Sciences, Kyoto University, Kyoto, Japan; ‖Laboratory for Immunopathology, RIKEN Research Center for Allergy and Immunology, Yokohama, Japan; and #Division of Experimental Immunology, Institute for Genome Research, University of Tokushima, Tokushima, Japan

Received for publication August 20, 2004. Accepted for publication November 17, 2004.

The costs of publication of this article were defrayed in part by the payment of page charges. This article must therefore be hereby marked *advertisement* in accordance with 18 U.S.C. Section 1734 solely to indicate this fact.

[1] This work was supported in part by Special Coordination Funds of the Ministry of Education, Culture, Sports, Science and Technology, the Japanese Government (MEXT), and by a grant-in-aid for Scientific Research from the MEXT.

[2] Address correspondence and reprint requests to Dr. Mitsuru Matsumoto, Division of Molecular Immunology, Institute for Enzyme Research, University of Tokushima, 3-18-15 Kuramoto, Tokushima 770-8503, Japan. E-mail address: mitsuru@ier.tokushima-u.ac.jp

[3] Abbreviations used in this paper: AIRE, autoimmune regulator; APECED, autoimmune-polyendocrinopathy-candidiasis ectodermal dystrophy; TEC, thymic epithelial cell; mTEC, medullary TEC; PHD, plant homeodomain; HEL, hen egg lysozyme; 3d-Tx mice, mice thymectomized 3 days after birth; SS, Sjögren's syndrome; Treg, immunoregulatory T cell; BM, bone marrow.

0022-1767/05/$02.00

of this finding was underscored by the fact that disease-causing missense mutations in PHD1 abolished its E3 ligase activity (10).

One important aspect of AIRE, in the context of autoimmunity, is its limited tissue expression in medullary thymic epithelial cells (mTEC) and cells of the monocyte-dendritic cell lineage of the thymus (13, 14). Both cell types are considered to play major roles in the establishment of self-tolerance by eliminating autoreactive T cells (negative selection) (1, 15) and/or by producing immunoregulatory T cells (Tregs), which prevent $CD4^+$ T cell-mediated organ-specific autoimmune diseases (16, 17). For this purpose, thymic epithelial cells (TECs) have been postulated to express a set of self-Ags encompassing all of the self-Ags expressed by parenchymal organs. Supporting this hypothesis, analysis of gene expression in the thymic stroma has demonstrated that mTECs are a specialized cell type in which promiscuous expression of a broad range of peripheral tissue-specific genes is an autonomous property (18). Aire in TECs has been suggested to regulate this promiscuous gene expression (19).

Fundamental roles of Aire in the elimination of autoreactive T cells in vivo have been demonstrated by the use of a TCR-transgenic mouse system (20). Mice expressing hen egg lysozyme (HEL) in pancreatic β cells driven by the rat insulin promoter were crossed with mice expressing TCR specific for HEL, and the fate of HEL-specific T cells was monitored in either the presence or absence of Aire. Remarkably, Aire-deficient TCR-transgenic mice showed almost complete failure to delete the autoreactive (i.e., HEL specific) T cells in the thymus (20). Because Aire-deficient mTEC showed a reduction in transcription of a group of genes encoding peripheral Ags analyzed by the gene-chip technique (19), it has been hypothesized that pathogenic autoreactive T cells could not be eliminated efficiently due to the reduced expression of corresponding target Ags in the Aire-deficient thymus (20). However, as this transgenic study did not demonstrate the effect of Aire loss on the thymic expression of HEL, there is still a lack of experimental evidence to connect the postulated roles of Aire in the transcriptional regulation of tissue-specific Ag expression with efficient elimination of autoreactive T cells. Thus, beyond transcriptional control of self-Ags in the thymus, other mechanisms of AIRE-dependent tolerance remain to be investigated. Furthermore, the effect of Aire deficiency on the production and/or function of Tregs has not yet been fully documented (19–21). Finally, the factors contributing to the complexity of the APECED phenotype (i.e., involvement of various target organs among patients) are unknown. Although intrafamilial variation in the clinical pictures suggests that factors other than the specific *AIRE* mutations might be involved in the disease process (22), this hypothesis cannot be easily proven in human subjects. To approach these issues, we have generated Aire-deficient mice by gene targeting. Identification of a target Ag associated with the tissue destruction caused by Aire deficiency together with strain-dependent target-organ specificity of the autoimmune disease has suggested unique properties of AIRE in the establishment and maintenance of self-tolerance.

Materials and Methods

Mice

Aire-deficient mice were generated by gene targeting. Briefly, the targeting vector was constructed by replacing the genomic *Aire* locus starting from exon 5 to exon 12 with the neomycin resistance gene (*neo*^{r}). The targeting vector was introduced into TT2 embryonic stem cells ($H\text{-}2^{b/k}$) (23), and the homologous recombinant clones were first identified by PCR and confirmed by Southern blot analysis. After the targeted cells had been injected into ICR 8 cell embryos (CLEA Japan), the resulting chimeric male mice were mated with C57BL/6 females to establish the germline transmission. C57BL/6 mice, BALB/c mice, and BALB/cA Jcl-*v* mice were purchased from CLEA Japan. The mice were maintained under pathogen-free conditions and handled in accordance with the Guidelines for Animal Experimentation of Tokushima University School of Medicine. The experiments were initiated when the mice were 8–12 wk of age.

Pathology

Formalin-fixed tissue sections were subjected to H&E staining, and two pathologists independently evaluated the histology without being informed of the condition of each individual mouse. Histological changes were scored as 0 (no change), 1 (mild lymphoid cell infiltration), or 2 (marked lymphoid cell infiltration).

Measurement of tear secretion

Measurement of tear secretion was performed as previously described (24, 25). Briefly, anesthetized mice were injected i.p. with 100 μl of pilocarpine hydrochloride (1 mg/ml) to stimulate tear production. Secreted tears were absorbed every 5 min with a cotton thread treated with a pH indicator phenol red (ZONE-QUICK; Menicon), and the length of the red portion of the thread was measured each time. Total length of the red portion of the thread during the first 20 min after pilocarpine injection was normalized by body weight.

ELISA and Western blot analysis

Various forms of recombinant α-fodrin were expressed with pGEX-4Ts plasmids (26). Western blot analysis and ELISA for the detection of auto-Abs against various forms of recombinant α-fodrin were performed with anti-mouse IgG Ab (Vector Laboratories), as described previously (25, 27–31). For the ELISA, absorbance values greater than the mean $\pm$ 3 SD in wild-type sera were considered positive. Western blot analysis of α-fodrin expression from the proteins extracted from the thymus and lacrimal glands was performed with mouse anti-α-fodrin mAb (Affiniti) and rabbit anti-AFN-A polyclonal Ab (25, 27–31).

Autoreactive responses against α-fodrin

For in vitro stimulation with α-fodrin, total splenocytes were stimulated with 10 μg/ml recombinant α-fodrin. For the last 8 h of the 32-h culture period, the cells were pulsed with [^{3}H]thymidine, and ^{3}H incorporation was determined as described previously (25).

Thymic stroma preparation

Thymic stroma was prepared as described previously with slight modification (32). Briefly, thymic lobes were isolated from three mice for each group and cut into small pieces. The fragments were gently rotated in RPMI 1640 medium (Invitrogen) supplemented with 10% heat-inactivated FCS (Invitrogen), 20 mM HEPES, 100 U/ml penicillin, 100 μg/ml streptomycin, and 50 μM 2-ME, hereafter referred to as R10, at 4°C for 30 min, and dispersed further with pipetting to remove the majority of thymocytes. The resulting thymic fragments were digested with 0.15 mg/ml collagenase IV (Sigma-Aldrich) and 10 U/ml DNase I (Roche Molecular Biochemicals) in RPMI 1640 at 37°C for 15 min. The supernatants that contained dissociated TECs were saved, whereas the remaining thymic fragments were further digested with collagenase IV and DNase I. This step was repeated twice, and the remaining thymic fragments were digested with collagenase IV, DNase I, and 0.1 mg/ml dispase I (Roche Applied Science) at 37°C for 30 min. The supernatants from this digest were combined with the supernatants from the collagenase digests, and the mixture was centrifuged for 5 min at 450 $\times$ *g*. The cells were suspended in PBS containing 5 mM EDTA and 0.5% FCS and kept on ice for 10 min. $CD45^-$ thymic stromal cells were then purified by depleting $CD45^+$ cells with MACS CD45 microbeads (Miltenyi Biotec) according to the manufacturer's instructions. The resulting preparations contained ~60% Ep-CAM^+ cells and <10% thymocytes (i.e., CD4/CD8 single-positive and CD4/CD8 double-positive cells), as determined by flow cytometric analysis.

RT-PCR

RNA was extracted from thymic stromal cells with High Pure RNA isolation kit (Roche Applied Science) and made into cDNA with cDNA Cycle kit (Invitrogen) according to the manufacturer's instructions. The following primer pairs for the *α-fodrin* gene were used: 5′-GCTTCAAGGAG CTCTCTACC-3′ and 5′-GCAGTTTGATTCCTTTCTCC-3′ (encompassing *α-fodrin* exons 1–3; accession no. XM_355324), 5′-CCAGCAGCAA CAATTTAATC-3′ and 5′-AGCAGATTCTGGACTCCAAT-3′ (encompassing the *α2-spectrin* exons 2–4; accession no. XM_207079), and 5′-GTG CAGAAATCAGCTGAGAA-3′ and 5′-GCTTGTGTTTCTTCCTCAGA-3′ (encompassing the *α2-spectrin* exons 24–27). PCR was conducted in a final volume of 20 μl with 1.5 U of ExTaq DNA polymerase (Takara Biomedicals)

and 250 nM each primer. Cycling conditions comprised a single denaturing step at 94°C for 10 min followed by 35 cycles of 94°C for 30 s, 60°C for 30 s, and 72°C for 1.5 min, followed by a final extension step of 72°C for 10 min. For *β-actin*, a single denaturing step at 94°C for 3 min was followed by 25 cycles of 94°C for 45 s, 50°C for 45 s, and 72°C for 1 min, followed by a final extension step of 72°C for 3 min (33).

Real-time PCR

Real-time PCR for quantification of *α-fodrin*, *Foxn1*, and tissue-specific Ag genes was conducted with thymic stroma cDNA prepared as described above. The primers and the probes are as follows. *α2-spectrin* primers: 5′-GACAGCCAGTGATGAGTCATACAAG-3′ and 5′-CACGGATTCG-GTCAGCATT-3′; *α2-spectrin* probe: 5′-FAM-ACCCCACCAACATCC AGAGCAAGC-3′; *Foxn1* primers: 5′-GACATGCACCTCAGCACTCT CTA-3′ and 5′-CTGATGTTGGGCATAGCTCAAG-3′; *Foxn1* probe: 5′-FAM- CCCGGCTCAAAGCCATTGGCTC-3′; *insulin* primers: 5′-AGA CCATCAGCAAGCAGGTC-3′ and 5′-CTGGTGCAGCACTGATCCAC-3′; *insulin* probe: 5′-FAM-CCCGGCAGAAGCGTGGCATT-3′; *salivary protein 1* primers: 5′-ACTCCTTGTGTTGCTTGGTGTTT-3′ and 5′-TCGACTGAATCAGAGGAATCAACT-3′; *salivary protein 1* probe: 5′-FAM-TTCACCAGCAGAATCAGCAGTTCCAGAA; *C-reactive protein* primers: 5′-TACTCTGGTGCCTTCTGATCATGA-3′ and 5′-GGCTTC TTTGACTCTGCTTCCA-3′; *C-reactive protein* probe: 5′-FAM-C AGCTTCTCTCGGACTTTTGGTCATGA-3′; *fatty acid binding protein* primers: 5′-CGTGTAGACAATGGAAAGGAGCT-3′ and 5′-AA GAATCGCTTGGCCTCAACT-3′; *fatty acid binding protein* probe: 5′-FAM-TCATTACCAGAAACCTCTCGGACAGCA-3′; *glutamic acid decarboxylase 67* primers: 5′-TCCTCCAAGAACCTGCTTTCC-3′ and 5′-GCTCCTCCCCGTTCTTAGCT-3′; *glutamic acid decarboxylase 67* probe: 5′-FAM-CCGACTTCTCCAACCTGTTTGCTCAAGA-3′. *Foxp3* expression was examined with cDNAs prepared from splenocytes ($CD4^+CD25^+$ or $CD4^+CD25^-$) and total thymus. The primers, the probes, and the reactions used for *Foxp3* and *Hprt* were those described previously (33, 34).

Thymus grafting

Thymus grafting was performed as previously performed (33). Briefly, thymic lobes were isolated from embryos at 14.5 days postcoitus, and then cultured for 4 days on Nucleopore filters (Whatman) placed on R10 containing 1.35 mM 2′-deoxyguanosine (Sigma-Aldrich). Five pieces of thymic lobes were grafted under the renal capsule of BALB/c *nude* mice. After 6–8 wk, reconstitution of peripheral T cells was determined by flow cytometric analysis with anti-CD4 (clone GK1.5; BD Pharmingen) and anti-CD8 (clone 53-6.7; BD Pharmingen) mAbs, and then the thymic chimeras were used for analysis.

Immunohistochemistry

Immunohistochemical analysis of the thymus was performed as described previously (35, 36). For the detection of auto-Abs, mouse serum was incubated with various organs obtained from Rag2-deficient mice. FITC-conjugated anti-mouse IgG Ab (Southern Biotechnology Associates) was used for the detection (33).

Isolation and functional analysis of Tregs

Spleen cell suspensions were stained with FITC-conjugated anti-CD25 (clone 7D4) and PE-conjugated anti-CD4 (clone H129.19) (BD Pharmingen), and sorted by FACS (ALTRA; Beckman Coulter) as described previously (37). The purity of the $CD25^-$ and $CD25^+CD4^+$ populations was >90 and 95%, respectively. Spleen cells sorted as described above were cocultured with RBC-lysed and irradiated (15 Gy) spleen cells (5×10^4) from wild-type mice as APC for 3 days in 96-well round-bottom plates in R10. Anti-CD3 mAb (clone 145-2C11) (Cedarlane Laboratories) at a final concentration of 10 μg/ml was added to the culture for stimulation, and ^3H incorporation during the last 6 h of culture was measured.

Results

Development of Sjögren's syndrome (SS)-like pathologic changes in exocrine organs from Aire-deficient mice

To investigate the roles of AIRE in the establishment and maintenance of self-tolerance in vivo, we generated Aire-null mutant mice. To this end, we deleted a large proportion of the known functional domains of *Aire* including SAND, PHD1, and PHD2 (6) (Fig. 1*A*). The correct targeted event was confirmed by Southern blot analysis and genomic PCR of material from the gene-targeted

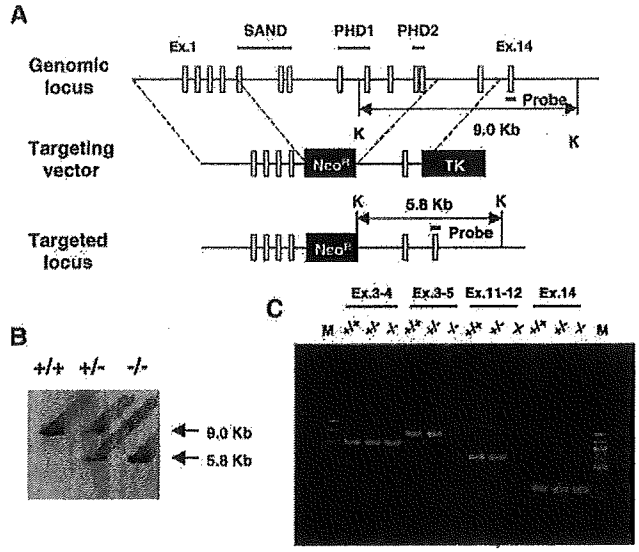

FIGURE 1. Generation of Aire-deficient mice. *A*, Targeted disruption of the gene encoding *Aire* by homologous recombination. K, *Kpn*I restriction site. *B*, Southern blot analysis of genomic DNA from offspring of heterozygous Aire-deficient mouse intercrosses. Tail DNA was digested with *Kpn*I and hybridized with a probe shown in *A*. *C*, Detection of genomic fragments of the *Aire* locus by PCR. Sequences spanning exons 5 and 12 were not amplified in tail DNA of homozygous Aire-deficient mice.

mice (Fig. 1, *B* and *C*). Offspring homozygous for Aire deficiency were born in the numbers expected from the heterozygous crossing, and homozygous Aire-deficient mice were grossly normal. Although both male and female homozygous Aire-deficient mice are fertile when crossed with wild-type mice, homozygous crossing produced offspring only occasionally (F. Kajiura and M. Matsumoto, unpublished observation). Total spleen cell numbers and total thymocyte numbers were indistinguishable between control and Aire-deficient mice. Flow cytometric analysis showed similar expression of B220, CD3, CD4, and CD8 in the spleen and thymus of control and Aire-deficient mice. Proliferative responses and Ig production from the B cells after various stimuli, and proliferative responses and IL-2 production from the T cells stimulated with anti-CD3 mAb, were also unchanged by the Aire deficiency (S. Sun and M. Matsumoto, unpublished observation).

To assess the impact of Aire deficiency on the breakdown of self-tolerance, we inspected various organs (i.e., salivary glands, lacrimal glands, thyroid, heart, lung, liver, stomach, pancreas, kidney, small intestine, testis, and ovary) from Aire-deficient mice of original mixed background (i.e., $H\text{-}2^{b/k} \times H\text{-}2^b$). The most marked changes were evident in the lacrimal glands (Fig. 2, *A* and *B*); all the Aire-deficient mice showed infiltration of many lymphoid cells in the lacrimal glands, whereas no such changes were observed in the control mice. We also observed infiltration of many lymphoid cells in the parotid glands (8 of 8 Aire-deficient mice) and submandibular glands (10 of 16 Aire-deficient mice) (Fig. 2*A*). Consistent with these SS-like pathologic changes in exocrine organs from Aire-deficient mice, secretion of tears per unit of mouse body weight was decreased in the affected mice (0.89 ± 0.33 mm/20 min/body weight (g) from control mice ($n = 5$) vs 0.46 ± 0.08 mm/20 min/body weight (g) from Aire-deficient mice ($n = 4$); $p < 0.05$). In 1 of 10 Aire-deficient mice, lymphoid cell infiltration in either the stomach or pancreas was also observed. There were no obvious pathologic changes in other organs from Aire-deficient mice during follow-up to the age of 8 mo.

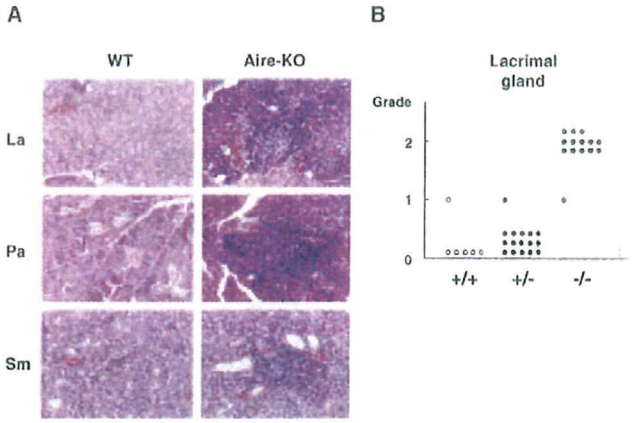

FIGURE 2. Development of organ-specific pathologic changes in Aire-deficient mice. *A*, Aire-deficient mice exhibited many infiltrating lymphoid cells in the lacrimal gland (La), parotid gland (Pa), and submandibular gland (Sm). In contrast, these changes were scarcely observed in control mice. Original magnification, ×100. *B*, Histological changes in H&E-stained tissue sections were scored as 0 (no change), 1 (mild lymphoid cell infiltration), or 2 (marked lymphoid cell infiltration). One mark corresponds to one mouse analyzed.

Autoreactive responses against α-fodrin in Aire-deficient mice

We have previously reported that NFS/*sld* mutant mice thymectomized 3 days after birth (3d-Tx) exhibit SS-like phenotypes with autoreactivity against α-fodrin, a ubiquitously expressed actin-binding protein (27, 38). Because of the similarity of SS-like phenotypes between Aire-deficient mice and the 3d-Tx-SS model, we investigated whether Aire-deficient mice exhibit autoreactivity against α-fodrin. We first tested the production of auto-Ab against various forms of recombinant α-fodrin in sera from Aire-deficient mice using Western blot analysis (Fig. 3, *A* and *B*). Sera from 3d-Tx mice showed reactivity predominantly against the JS-1 fragment (27). Four of five Aire-deficient mice showed reactivity against 2.7A, and two mice showed reactivity against 3′DA (Fig. 3*B*). Sera from control mice showed no such reactivities. Production of auto-Ab against α-fodrin in Aire-deficient mice was also evaluated by ELISA using additional forms of recombinant α-fodrin (31) and larger numbers of mice. Ten of 11 Aire-deficient mice showed significantly higher reactivities against at least one form of recombinant α-fodrin fragment compared with those from 11 control mice (Fig. 3*C*). Interestingly, each Aire-deficient mouse showed reactivity against different forms of α-fodrin.

We also confirmed the development of autoimmunity against α-fodrin using splenocytes from Aire-deficient mice (25). Such splenocytes cultured with recombinant α-fodrin showed significant proliferative responses; four Aire-deficient mice tested showed a response to 2.7A, but not to JS-1, whereas no such reactivities were observed from age-matched control mice (Fig. 4).

Unrepressed expression of corresponding target Ag in Aire-deficient thymus

The mechanism controlling the thymic microenvironment necessary for the establishment of self-tolerance in an Aire-dependent manner is of considerable interest. It has been suggested that "promiscuous" expression of a broad range of peripheral tissue-specific genes by TECs is essential for establishing self-tolerance (18), and Aire has been implicated in the control of this promiscuous gene expression through a transcriptional mechanism (19). Supporting this notion, real-time PCR has revealed that expression of *insulin*

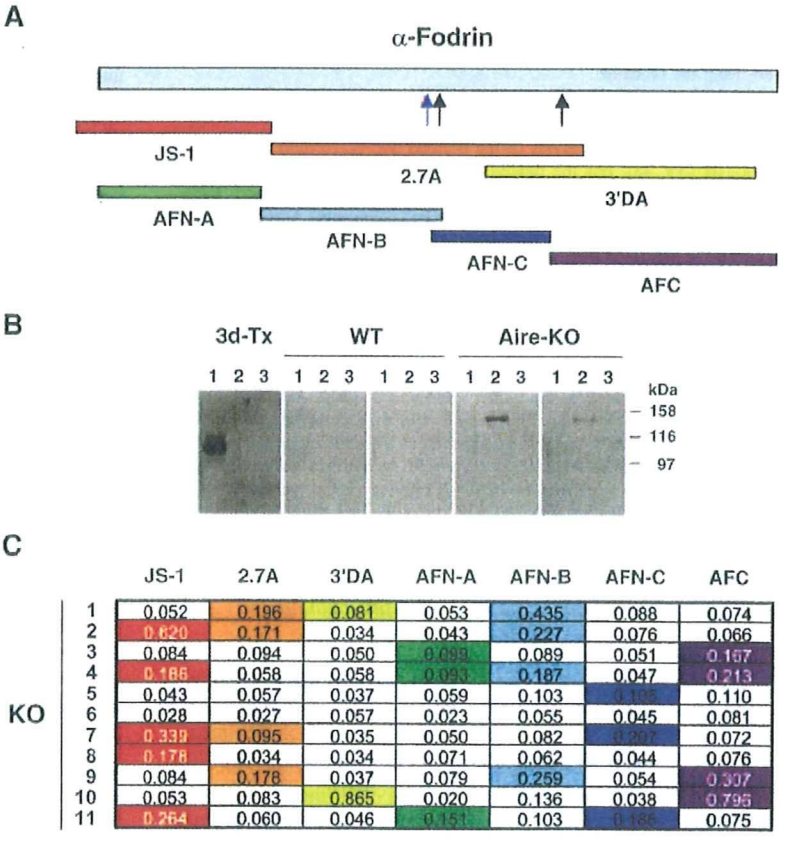

FIGURE 3. Production of auto-Abs against α-fodrin in Aire-deficient mice. *A*, Schematic representation of α-fodrin. Black arrows and a blue arrow show the sites of cleavage by caspase 3 and calpain, respectively. *B*, Western blot analysis for recombinant α-fodrin with Aire-deficient mouse sera. Representative results from two mice from both wild-type and Aire-deficient mice are shown. Serum from NFS/*sld* mutant 3d-Tx mice reacted predominantly with the JS-1 fragment. 1, JS-1; 2, 2.7A; 3, 3′DA. *C*, Detection of auto-Abs against various forms of α-fodrin in sera from Aire-deficient mice using ELISA. Absorbance values greater than the mean ± 3 SD in wild-type mouse sera were considered positive and are colored.

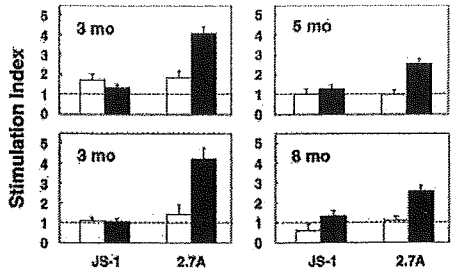

FIGURE 4. Autoreactive responses against α-fodrin by splenocytes from Aire-deficient mice. Proliferative responses of total splenocytes against two forms of recombinant α-fodrin (shown in Fig. 3*A*) were determined, and stimulation indices are demonstrated from control mice (open bars) and Aire-deficient mice (filled bars). Ages of the mice used are indicated.

and *salivary protein 1* was significantly reduced in the Aire-deficient thymic stroma (Fig. 5*A*). Because Aire-deficient mice developed autoimmunity against the defined target Ag, α-fodrin, we examined whether the expression of α-fodrin mRNA in the thymic stroma is changed in Aire-deficient mice. Using real-time PCR together with semiquantitative RT-PCR with three sets of primers encompassing the entire coding region of *α-fodrin*, we detected unrepressed *α-fodrin* expression from Aire-deficient thymic stroma when compared with that from control thymic stroma (Fig. 5, *A* and *B*); this was observed under the condition where the expression of *Foxn1*, which encodes a transcription factor involved in thymus development (39), was indistinguishable between the samples (Fig. 5*A*). Thus, our results suggest that Aire regulates self-tolerance beyond the transcriptional control of self-protein expression in the thymus, at least against this ubiquitously expressed protein.

To test whether autoreactivity against α-fodrin is associated with the development of inflammatory lesions in exocrine organs from Aire-deficient mice, we performed Western blot analysis using proteins extracted from the lacrimal glands. Both lacrimal glands and thymus from younger Aire-deficient mice (i.e., 3 mo) contained larger quantities of intact form α-fodrin (240 kDa) than the cleaved form (150 kDa), as observed for proteins from the control mice (Fig. 6*A*); this was demonstrated with two different kinds of Abs recognizing the C-terminal half (anti-α-fodrin mAb) and N-terminal half (anti-AFN-A polyclonal Ab) of α-fodrin. However, lacrimal glands from some aged Aire-deficient mice (i.e., 8 mo) contained a reduced amount of the intact form (Fig. 6*B*), although no detectable changes in α-fodrin expression in the thymus were observed in either form or quantity. This result suggests that autoreactivity against α-fodrin is associated with the pathogenetic process responsible for destruction of the lacrimal glands in this SS-like model, as observed in 3d-Tx-SS model (27, 38).

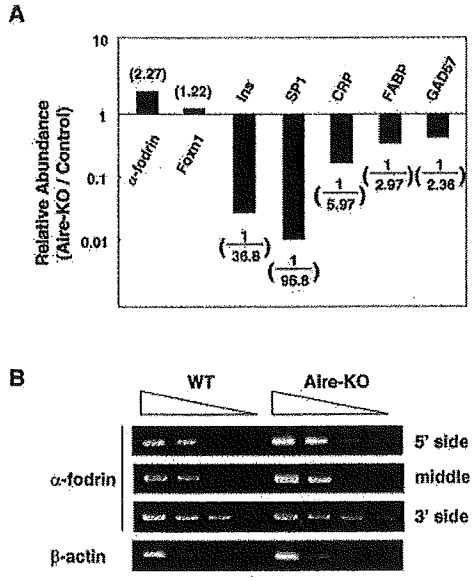

FIGURE 5. Unrepressed target Ag expression from Aire-deficient thymus. *A*, Real-time PCR for *α-fodrin*, *Foxn1*, and peripheral tissue-specific genes (i.e., Ins, *insulin*; SP1, *salivary protein 1*; CRP, *C-reactive protein*; FABP, *fatty acid-binding protein*; GAD67, *glutamic acid decarboxylase 67*) was performed using thymic-stroma RNAs from control and Aire-deficient mice. *Hprt* expression level was used as an internal control. Relative abundance of each gene was calculated from the ratio between the values from control thymus and those from Aire-deficient thymus (e.g., *insulin/Hprt* value from Aire-deficient mice was divided by *insulin/Hprt* value from control mice) and is shown in parentheses. One representative result from a total of three repeats is shown. *B*, Semiquantitative RT-PCR for *α-fodrin* was performed using thymic-stroma RNAs from control and Aire-deficient mice. *β-Actin* was used to verify equal amounts of RNAs in each sample. Three sets of primers encompassing the entire coding region of *α-fodrin* were used for detection. One representative result from a total of three repeats is shown.

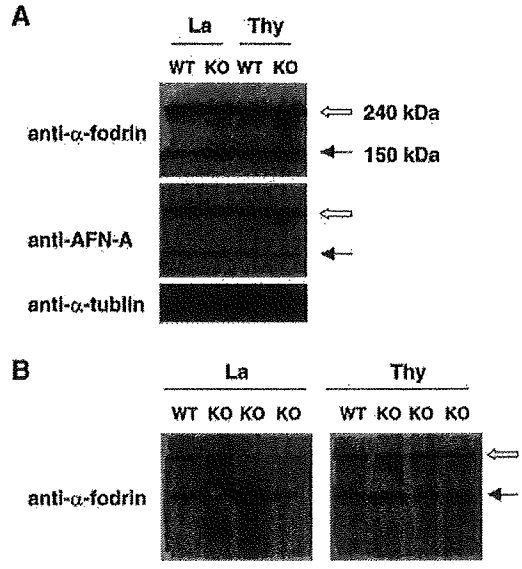

FIGURE 6. Autoreactivity against α-fodrin is associated with the pathogenetic process responsible for destruction of the lacrimal glands. *A*, Proteins extracted from the lacrimal glands and thymus of 3-mo-old mice were subjected to Western blot analysis using two different kinds of Abs recognizing the C-terminal half (anti-α-fodrin Ab, *top*) and N-terminal half (anti-AFN-A Ab, *center*) of α-fodrin. Open and filled arrows indicate the 240-kDa intact form and 150-kDa cleaved form of α-fodrin, respectively. The same blot was probed with anti-α-tubulin Ab (*bottom*). La, lacrimal gland; Thy, thymus. *B*, Proteins were extracted from the lacrimal glands and thymus of 8-mo-old mice. Western blot analysis was performed as shown in *A*. Lacrimal glands from some of the Aire-deficient mice showed a markedly reduced amount of the intact form (*left panel*, third and fourth lanes), although Aire-deficient thymus showed no detectable changes in α-fodrin expression in terms of form or quantity compared with control thymus (*right panel*). Open and filled arrows indicate the 240-kDa intact form and 150-kDa cleaved form of α-fodrin, respectively.

Loss of Aire in the thymic stroma is responsible for the breakdown of self-tolerance

Despite the predominant Aire expression in TECs, thymic structure was not apparently affected by the absence of Aire. Results of H&E staining as well as immunohistochemistry with the lectin *Ulex europaeus* agglutinin 1 (40) and ER-TR5 mAb (41), both recognizing a subset of mTEC, were indistinguishable between control and Aire-deficient mice (F. Kajiura, T. Ueno, Y. Takahama, and M. Matsumoto, unpublished observation). Organization of dendritic cells in the thymus identified with the mAb CD11c was also unaffected by Aire deficiency. Thus, Aire may not affect thymic organogenesis. Alternatively, relatively low frequencies of Aire-expressing cells among mTECs may account for the apparently normal thymic structure in Aire-deficient mice.

To investigate the impact of Aire deficiency in the thymic microenvironment, we generated thymic chimeras. Thymic lobes were isolated from control and Aire-deficient embryos of mixed background (H-$2^{b/k}$ × H-2^{b}) and cultured for 4 days in the presence of 2′-deoxyguanosine to eliminate thymocytes. Such thymic lobes did not contain any live thymocytes, as determined by flow cytometric analysis and Western blot analysis with anti-lck Ab (33). The lobes were then grafted under the renal capsule of BALB/c *nude* mice (H-2^{d}). Grafting of both control and Aire-deficient embryonic thymus induced T cell maturation in BALB/c *nude* mice at the periphery to a similar extent: $CD4^+$ T cells plus $CD8^+$ T cells were 12.5 ± 2.2% in *nude* mice grafted with control thymus ($n = 6$), compared with 12.3 ± 1.6% in *nude* mice grafted with Aire-deficient thymus ($n = 7$). It is important to note that the mature T cells produced de novo in both cases originated from Aire-sufficient *nude* mouse bone marrow (BM). Remarkably, histological examination of Aire-deficient thymus-grafted mice revealed infiltration of many lymphoid cells in the liver (mainly in the portal area) and pancreas (interlobular periductal and perivascular areas near islets) (Fig. 7, *A* and *B*). In contrast, we observed few such changes in control thymus-grafted mice.

To confirm that T cells developing in a thymic microenvironment without Aire are autoreactive per se, we injected splenocytes obtained from BALB/c *nude* mice grafted with Aire-deficient thymus into another group of BALB/c *nude* mice. We observed similar lymphoid cell infiltration in the liver of the recipient mice, whereas injection of splenocytes obtained from *nude* mice grafted with control thymus induced no such changes in the recipient mice (Fig. 7*B*). These results clearly indicate the significance of Aire as a thymic stromal element required for the establishment of self-tolerance.

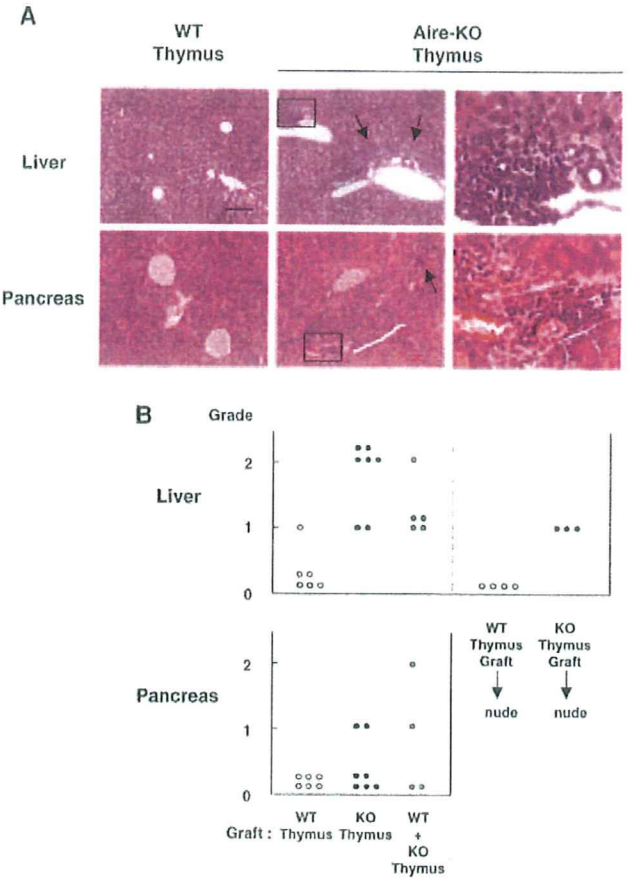

FIGURE 7. Thymic stromal elements in Aire-deficient mice are responsible for the development of autoimmunity. *A*, BALB/c *nude* mice grafted with Aire-deficient embryonic thymus (*middle panels*), but not with control embryonic thymus (*left panels*), developed an autoimmune disease phenotype in the liver and pancreas. The indicated areas are magnified in the *right panels*. Arrows indicate lymphoid cell infiltration. The scale bar corresponds to 100 μm. *B*, Many Aire-deficient thymus-grafted BALB/c *nude* mice exhibited lymphoid cell infiltration in the liver (*top*) and pancreas (*bottom*). In contrast, such changes were scarcely observed in mice grafted with control thymus. BALB/c *nude* mice grafted with both Aire-deficient thymus and control thymus showed significant pathological changes. Injection of splenocytes from BALB/c *nude* mice grafted with Aire-deficient thymus, but not with control thymus, into another group of BALB/c *nude* mice induced lymphoid cell infiltration in the liver of the recipient mice. Histological changes in H&E-stained tissue sections were scored as shown in Fig. 2*B*. One mark corresponds to one mouse analyzed.

Impaired regulation of autoreactivity in the absence of Aire

There is accumulating evidence that T cell-mediated dominant control of autoreactive T cells represents an important mechanism for the maintenance of immunologic self-tolerance (16, 17). We investigated whether loss of Aire in the thymus has a major impact on the production and/or function of Tregs. Spleen and thymus from adult Aire-deficient mice contained similar percentages as well as total numbers of $CD4^+CD25^+$ T cells compared with those from control mice (Fig. 8*A*). Real-time PCR for quantification of *Foxp3* mRNA (34, 42, 43) did not show any reduction of Tregs in the spleen of Aire-deficient mice (Fig. 8*B*). Expression of *Foxp3* in the whole thymus was also comparable between control mice and Aire-deficient mice (*Foxp3/Hprt* from wild-type mice = 1.8 vs *Foxp3/Hprt* from Aire-deficient mice = 2.4).

Recently, it has been demonstrated that functional alterations of Tregs could contribute to the development of autoimmune disease. A significant decrease in the effector function of $CD4^+CD25^+$ T cells from peripheral blood of patients with multiple sclerosis has been reported (44). It is of particular interest that the suppressor function of $CD4^+CD25^+$ T cells has been demonstrated to be defective in patients with autoimmune polyglandular syndrome type II, which is phenotypically closely related to APECED (also called autoimmune polyglandular syndrome type I) but whose pathogenesis is currently unknown (45). It is therefore important to test the function of Tregs from Aire-deficient mice. $CD4^+CD25^+$ T cells isolated from Aire-deficient mice dose-dependently suppressed [^{3}H]thymidine uptake by naive T cells cocultured in vitro with an efficiency nearly identical to that of $CD4^+CD25^+$ cells from control mice (Fig. 8*Ca*). This was also the case when responder cells ($CD4^+CD25^-$ cells) isolated from Aire-deficient mice were used for the assay (Fig. 8*Cb*). Thus, Aire does not have a major impact on the production and/or function of Tregs, at least as assessed in those assays.